AN ABSTRACT OF THE THESIS OF

Julie A. Auxier for the degree of Master of Science in Chemical Engineering presented on November 30, 2012

Title: Retention of Protein Repulsive Character and Antimicrobial Activity of PEO Brush Layers following Nisin Entrapment

Abstract approved:

_____

Joseph McGuire

Nisin, an amphiphilic, antimicrobial peptide, has been shown to integrate into the hydrophobic inner region of poly(ethylene oxide) (PEO) brush layers; however, the presence of integrated nisin may compromise the protein repulsive character of the PEO layer. In particular, the introduction of fibrinogen to nisin-loaded brush layers has been observed to cause changes consistent with partial elution of nisin and/or location of fibrinogen at the interface. Questions surrounding the possibility of fibrinogen adsorption warrant further investigation, as the location of procoagulant proteins at a peptide-loaded PEO layer would significantly reduce the viability of a medical device coating based on such an approach. In this work, the preferential location of fibrinogen at PEO brush layers was investigated by: detection of FITC-labeled fibrinogen after sequential introduction of nisin and labeled fibrinogen; measurement of changes in the zeta potential of PEO coated and uncoated surfaces following nisin, fibrinogen, and/or buffer challenges; and evaluation of adsorption and elution kinetics in label-free, sequential adsorption experiments using optical waveguide lightmode

spectroscopy (OWLS). PEO layers were constructed through radiolytic grafting of Pluronic® F108 or F68 onto silanized silica surfaces producing long-chain or short-chain PEO layers, respectively. Adsorption results indicated that sequential introduction of nisin and fibrinogen to PEO brush layers, based on F108, does not result in fibrinogen adsorption beyond that expected for a nisin-free PEO layer. No evidence of nisin entrapment in fibrinogen-repellent F68 layers was recorded. Low-level fibrinogen adsorption observed at F68 layers following the introduction of nisin was determined to be a result of nisin adsorption at (uncoated) defect regions on the surface. In conclusion, retention of PEO layer capacity for protein repulsion after nisin entrapment is owing to a steric repulsive barrier provided by PEO segments extending beyond the level of entrapped nisin.

It was then hypothesized that the immobilized, pendant PEO chains will inhibit exchange of entrapped nisin by competing proteins, and therefore prolong nisin activity retention. In order to evaluate nisin function following its entrapment, the antimicrobial activity of nisin-loaded, F108-coated silica surfaces was evaluated against the Gram-positive indicator strain, *Pediococcus pentosaceous*. The retained biological activity of these nisin-loaded layers was evaluated after incubation in the presence of bovine serum albumin (BSA), for contact periods up to one week. Surfaces were withdrawn at selected times and placed on plates inoculated with *P. pentosaceous* to measure kill zone radius in order to quantify nisin activity. In the presence of BSA, F108-coated surfaces retained more antimicrobial activity than the uncoated, hydrophobic surfaces. These results strongly suggest that PEO brush layers may serve as a viable drug storage platform due to the retained non-fouling character after bioactive peptide entrapment and the prolonged peptide activity in the presence of other proteins.

Retention of Protein Repulsive Character and Antimicrobial Activity of PEO Brush Layers following Nisin Entrapment

by

Julie A. Auxier

A THESIS

submitted to

Oregon State University

in partial fulfillment of
the requirements for the
degree of

Master of Science

Presented November 30, 2012
Commencement June 2013

Master of Science thesis of Julie A. Auxier presented on November 30, 2012.

APPROVED:

_____

Major Professor, representing Chemical Engineering

_____

Head of the School of Chemical, Biological, and Environmental Engineering

_____

Dean of the Graduate School

I understand that my thesis will become part of the permanent collection of Oregon State University libraries. My signature below authorizes release of my thesis to any reader upon request.

_____

Julie A. Auxier, Author

ACKNOWLEDGEMENTS

My experience at Oregon State University working in the Biointerfaces and Biomaterials laboratory has been a grand adventure of personal and professional growth. I have been most fortunate to have been a part of such a supportive environment and even more fortunate to have Dr. Joseph McGuire for a mentor. Dr. McGuire has served as my advisor for the past five years through my undergraduate and graduate career. He has helped me in professional and personal development and has been a constant source of wisdom. I am profoundly grateful for all his guidance and support.

I also extend my sincere gratitude to Dr. Karl Schilke, who I will forever know as Rat. Since my first summer as an intern, he has been an invaluable source of knowledge and advice. I attribute much of the research and scientific intuition that I have developed to Rat. I appreciate all the discussions, after hours assistance, instruction, and humor along the way.

I have had the distinct pleasure of learning from Dr. Tom Shelhammer and Jeff Clawson. They have been instrumental in developing my interest in and knowledge of food and fermentation science. Their instruction has enlightened me of a whole new array of possibilities and provided renewed purpose and direction in my career.

The various members of the McGuire lab with whom I have worked and on whom I have relied must also be mentioned, particularly: Justen Dill, Andy Sinclair, Matt Ryder, Keely Heintz, Lars Bowlin, and Josh Snider. This work would not have been as successful without their help. The McGuire lab group fosters a collaborative nature that is most admirable. I will bring the values learned in the lab with me wherever my career takes me.

I would also like to thank my family for their unending support; I am so fortunate to have such a strong support system. I am also extremely grateful to all those who have kept me sane during this endeavor. To those who encouraged me when the outlook was bleak, who helped me through late nights and long weekends, and who restored my confidence when needed, I thank you and am indebted to you for your kindnesses.

CONTRIBUTION OF AUTHORS

Dr. Joseph McGuire and Dr. Karl Schilke supervised and edited the manuscripts presented in this thesis. Frequent discussions guided the work's progress and ultimately contributed to this thesis. Dr. McGuire and Dr. Schilke also provided insight and guidance on OWLS data interpretation. Justen Dill contributed to OWLS experimentation and data collection.

Dr. Schilke provided training and assistance in surface modification techniques in addition to helpful critique on experimental troubleshooting. Andy Sinclair assisted with the initial activity test. Lars Bowlin and Josh Snider assisted with MIC determination. Justen Dill assisted with CFU determination.

TABLE OF CONTENTS

TABLE OF CONTENTS (Continued)

LIST OF FIGURES

LIST OF APPENDIX FIGURES

LIST OF APPENDIX FIGURES (Continued)

Figure Page

DEDICATION

For the motivators who have inspired me to persevere

and the educators who have enabled me to succeed.

RETENTION OF PROTEIN REPULSIVE CHARACTER AND ANTIMICROBIAL ACTIVITY OF PEO BRUSH LAYERS FOLLOWING NISIN ENTRAPMENT

CHAPTER 1

GENERAL INTRODUCTION

Nisin is a small (3.4 kDa) cationic, amphiphilic peptide that is an effective inhibitor of Gram-positive bacteria. Its potential use in anti-infective coating strategies has motivated interest in its adsorption and function at biomaterial interfaces. Nisin adsorption and various aspects of its behavior at PEO-coated surfaces have been described through ellipsometry, circular dichroism and assays of antibacterial activity, zeta potential, and TOF-SIMS. Indirect evidence provided in these studies suggests that introduction of fibrinogen to nisin-loaded PEO layers causes changes consistent with partial elution of nisin and/or location of fibrinogen at the interface. Questions surrounding the possibility of fibrinogen adsorption warrant further investigation, as location of procoagulant proteins at a peptide-loaded PEO layer would significantly reduce the viability of a medical device coating based on such an approach.

Blood protein repulsion is largely independent of PEO chain length, when the chain density is sufficiently high ($> 0.2/nm^2$) to produce a brush configuration. Thus, it is fair to expect that after adsorption of nisin to a PEO brush and subsequent elution of loosely held peptides, the PEO segments extending beyond the level of entrapped nisin will again be mobile and provide a steric repulsive barrier to protein adsorption. In Chapter 2, direct and quantitative evidence is provided, from several complementary methods, that sequential

introduction of nisin and fibrinogen to a PEO brush layer does not result in location of fibrinogen at that layer, in line with expectations.

Given that the protein repelling capacity of a PEO layer after nisin entrapment is retained, it was hypothesized that the antimicrobial activity of nisin at the surface will be prolonged through its entrapment, owing to inhibition of nisin exchange by competing proteins in solution by the pendant PEO chains. Chapter 3 provides an evaluation of nisin function following its entrapment. In particular, the antimicrobial activity of nisin-loaded, uncoated hydrophobic and nisin-loaded F108-coated silica surfaces was evaluated against the Gram-positive indicator strain, *Pediococcus pentosaceous*.

In addition to supplementary descriptions of surface modification, and antibacterial activity of free and entrapped nisin against *P. pentosaceus* and *S. epidermidis*, two finished manuscripts to which the author made significant contributions are included in the appendices. Appendix C (Ryder *et al*., *J. Colloid Interface Sci.* 350:194-199, 2010) is the published report that motivated the research described in this thesis, in which detection of zeta potential was used along with an anti-fibrinogen ELISA assay to begin to describe the sequential adsorption behavior of nisin and fibrinogen at PEO layers. Appendix D (Dill *et al*., *J. Colloid Interface Sci.*, submitted October 2012) provides surface analytical evidence that nisin entrapment in PEO is characterized by its location within the hydrophobic inner region of the PEO brush layer, and not at the underlying surface. The hydrophobic inner region of a PEO brush based on F108 is sufficient for peptide entrapment purposes, while that of a brush based on the shorter PEO chains of F68 is not sufficient for peptide entrapment.

NISIN INTEGRATION AND FIBRINOGEN REPULSION AT PENDANT PEO LAYERS

Julie A. Auxier, Justen K. Dill, Karl F. Schilke, Joseph McGuire*

School of Chemical, Biological and Environmental Engineering, Oregon State University, Corvallis, OR 97331

*Corresponding author:

Gleeson Hall Rm. 102
Oregon State University
Corvallis, OR 97331 USA
E-mail: *joseph.mcguire@oregonstate.edu*
Telephone: 1-541-737-6306
Fax: 1-541-737-4600

CHAPTER 2

NISIN INTEGRATION AND FIBRINOGEN REPULSION AT PENDANT PEO LAYERS

Abstract

Nisin, an amphiphilic, antimicrobial peptide, has been shown to integrate into polyethylene oxide (PEO) brush layers; however, the presence of integrated nisin may compromise the protein repulsive character of the PEO layer. The introduction of fibrinogen to nisin-loaded brush layers has been observed to cause changes consistent with partial elution of nisin and/or location of fibrinogen at the interface. Preferential location of fibrinogen on modified surfaces was investigated via FITC-labeling and optical waveguide lightmode spectroscopy (OWLS). Results from each technique indicate that fibrinogen does not adsorb substantially to PEO-coated surfaces, even when the layer is loaded with nisin.

Keywords: nisin adsorption; fibrinogen repulsion; Pluronic® F108; PEO brush layer; optical waveguide lightmode spectroscopy; sequential adsorption

2.1 Introduction

Coating surfaces with poly(ethylene oxide) (PEO) based polymers has been shown to mediate undesirable protein location at interfaces [1-7]. Blood protein repulsion is largely independent of PEO chain length, when the chain density is sufficiently high (> 0.2/nm^2) to produce a brush configuration [8-11]. Pluronic® copolymers, containing a poly(propylene oxide) (PPO) center block (PEO-PPO-PEO), form self-assembled brush layers and have been shown to significantly repel relevant blood proteins, such as fibrinogen and albumin [1, 7, 10, 12-14]. Because fibrinogen is an essential precursor for platelet aggregation, it has been studied as a model protein. Protein adsorption at an interface is subject to conformational changes whereby the protein may become irreversibly or reversibly bound to the surface [15, 16]. These changes at the surface are consequently time dependent and further adsorption may exhibit "history dependent" behavior [17]. Dill *et al*. demonstrated that Pluronic® F108 PEO brush layers do not demonstrate history dependence owing to the layer's protein repulsive character [14].

These PEO layers may be given bioactive functionality by incorporation of bioactive peptides, such as the small, cationic, amphilphilic peptide, nisin [18]. Nisin is an antimicrobial peptide effective against Gram-positive bacteria [19]. Nisin associates at lipid vesicles, but will do so more strongly when lipid II is present in the membrane [20, 21]. Synthesis of peptidoglycan, the polymer that strengthens bacterial cell walls, is inhibited when nisin binds to lipid II, thereby increasing membrane permeabilization and allowing nisin to form highly specific pores [19, 22]. Nisin has been well characterized and so was chosen as a model peptide for this study.

The adsorption of nisin and its resistance to elution by fibrinogen at PEO-coated surfaces have been examined through ellipsometry [7] and zeta potential [1]. These studies

indicate that introduction of fibrinogen to nisin-loaded PEO layers causes changes consistent with partial elution of nisin and/or location of fibrinogen at the interface. Questions surrounding the possibility of fibrinogen adsorption warrant further investigation, as preferential location of procoagulant proteins at a peptide-loaded PEO layer would significantly reduce the viability of a medical device coating based on such an approach.

Despite PEO brush layers' generally protein-repulsive character, theory predicts that sufficiently small proteins may instead be integrated into PEO brushes [23]. Thus, it is fair to hypothesize that, with nisin adsorption in a brush, after the outermost peptides are eluted, the PEO segments extending beyond the level of entrapped nisin will again be mobile and provide a steric repulsive barrier to blood protein adsorption (Figure 2.1). Based on zeta potential and an anti-fibrinogen ELISA assay, Ryder *et al*. tentatively concluded that nisin is partially eluted from PEO layers in the presence of fibrinogen, but the steric repulsion of the layer was retained [1]. A later study of nisin and fibrinogen adsorption using TOF-SIMS was in qualitative agreement with this conclusion [24]. Here direct and quantitative evidence is provided, from several complementary methods, that validates the working hypothesis.

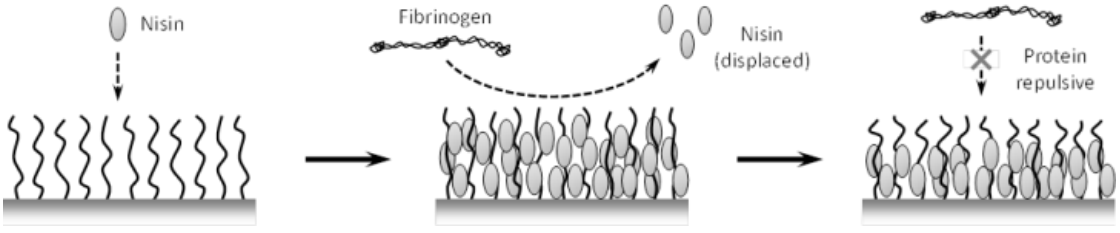

Figure 2.1: Nisin has been shown to integrate into an immobilized PEO brush. It is expected that upon contact with blood proteins, outermost nisin will elute from the PEO allowing the exposed PEO to regain repulsive character.

2.2 Materials and Methods

2.2.1 Surface modifications and PEO coatings

Silica microspheres (1 μm, Fiber Optic Center, New Bedford, MA) were cleaned and silanized with trichlorovinylsilane (TCVS) in anhydrous $CHCl_3$, as described by Ryder *et al.* [3]. SiO_2-coated sensors for optical waveguide lightmode spectroscopy (OWLS 210, MicroVacuum, Budapest, Hungary) were cleaned with chromosulphuric acid and silanized at 25 °C with TCVS vapor. TCVS-modified surfaces were coated by adsorption of 10 mg/mL Pluronic® F108 triblocks (BASF, Mount Olive, NJ) in 10 mM sodium phosphate buffer with 150 mM NaCl, pH 7.4 (PBS) or Pluronic®F68 (BASF, Mount Olive, NJ), and then γ-irradiated (^{60}Co, 0.3 Mrad) to covalently stabilize the PEO brush layers [1, 8, 9, 24]. The process is summarized in Figure 2.2a.

2.2.2 Adsorption of nisin and fibrinogen

Solutions of nisin (3.4 kDa, 0.5 mg/mL, Prime Pharma, Gordons Bay, South Africa), plasminogen-free human fibrinogen (340 kDa, 1 mg/mL, Sigma-Aldrich), and fluorescein isothiocyanate (FITC)-labeled human fibrinogen (1 mg/mL, Molecular Innovations, Novi, MI) in PBS were made and filtered (0.2 μm) immediately before use.

TCVS-modified or PEO triblock-coated surfaces were rinsed thrice with PBS, and then individually or sequentially contacted with nisin and/or fibrinogen solutions (Figure 2.2b). The amount of fibrinogen adsorption at surfaces was analyzed by the absorbance of fluoroscein from FITC-labeled fibrinogen, zeta potential, and OWLS, as described below.

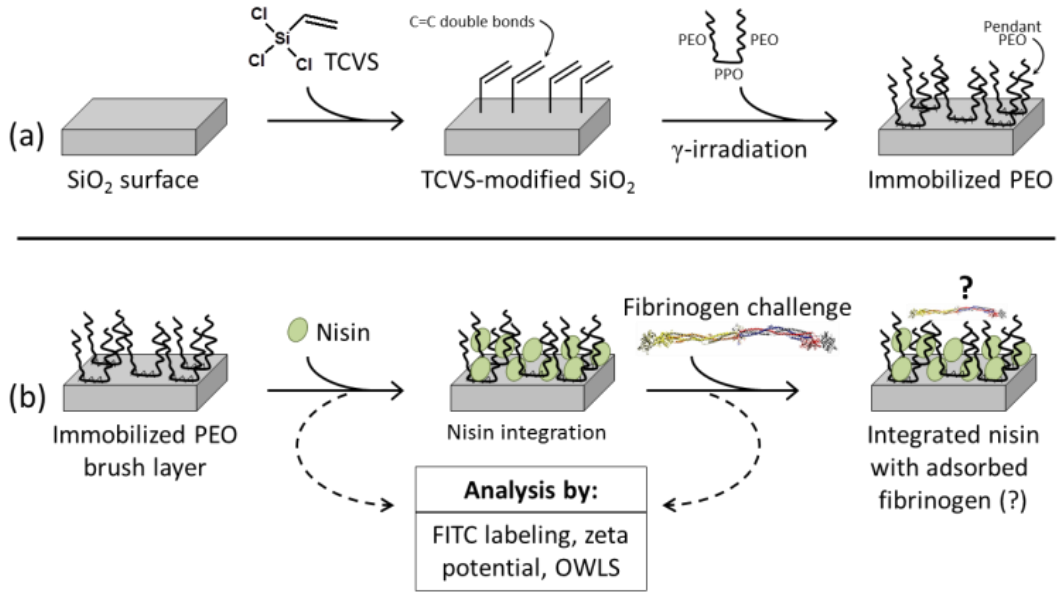

Figure 2.2: a) Silica modified with TCVS, followed by adsorption and irradiation of PEO-PPO-PEO triblocks to produce a stable, pendant PEO brush. b) Nisin integration into an immobilized PEO brush, followed by challenge with fibrinogen. Analysis was performed with FITC labeling, zeta potential, and OWLS techniques.

2.2.3 Quantification of FITC-labeled fibrinogen adsorbed on microspheres

Silica microspheres, with and without F108 coatings, were incubated with nisin (0.05 mg/mL) in PBS or protein-free buffer for 4 h, then rinsed thrice with PBS. The microspheres were then incubated with FITC-labeled fibrinogen (Molecular Innovations, FIB-FITC-909) solution (or buffer) overnight and rinsed thrice with PBS. The microspheres were dissolved in hot (80-100 °C) 1N NaOH, and the absorbance at 490 nm was used to calculate the mass of adsorbed FITC-labeled fibrinogen [25].

2.2.4 Zeta potential of microsphere suspensions

Zeta potential measurements (ZetaPALS, Brookhaven, Holtsville, NY) on F108 and F68 modified microspheres were conducted according to Ryder *et al.* [1]. Microspheres were incubated with nisin (0.5 mg/mL in PBS) for 1 h, thoroughly rinsed, and zeta potential measured. The samples were then challenged with 10 mM PBS with 150 mM NaCl solution

(denoted as “buffer”) or 1 mg/mL fibrinogen solution from human plasma (Lot: 059K7550, PID# F4883-500mg, SIGMA) for 1 h. Prior to testing, each sample was centrifuged and rinsed with water to remove fibrinogen, nisin, and salts from solution.

2.2.5 Optical waveguide lightmode spectroscopy (OWLS)

OWLS provides real time, label-free detection of protein adsorption on waveguide sensor chips [26]. TCVS-treated OWLS sensors, with and without γ-stabilized F108 coatings, were equilibrated in PBS overnight. After a steady baseline was achieved, 0.5 mg/mL nisin in PBS was injected into the flow loop and passed over the sensor for 30 min (50 µL/min). The sensor was then rinsed with PBS for 30 min, after which fibrinogen (1 mg/mL) was injected into the flow loop for 30 min. The sensors were then rinsed with flowing PBS for 30 min. Protein-free PBS was substituted for the protein solutions as appropriate.

2.3 Results and Discussion

2.3.1 Quantification of FITC-labeled fibrinogen on microspheres

The surface loading of adsorbed FITC-fibrinogen was estimated from the measured A_{490} and the manufacturer-specified F/P ratio of the fluorescein-labeled protein in the dissolved silica solution. The results, normalized to the negative control (hydrophobic TCVS silica), are presented in Figure 2.3. Qualitatively, the presence of FITC-labeled fibrinogen is clearly visible as a yellow tint on the microspheres without PEO coatings, while the PEO coated surfaces exhibit much less color. Quantitatively, significantly less FITC-fibrinogen adsorbed on surfaces coated with PEO by immobilization of Pluronic® F108. Further, the presence of nisin did not significantly affect the adsorption of FITC-fibrinogen on either PEO-coated or uncoated microspheres. The protein-repellent nature of the PEO coating is apparently unaffected by the presence of nisin in the brush.

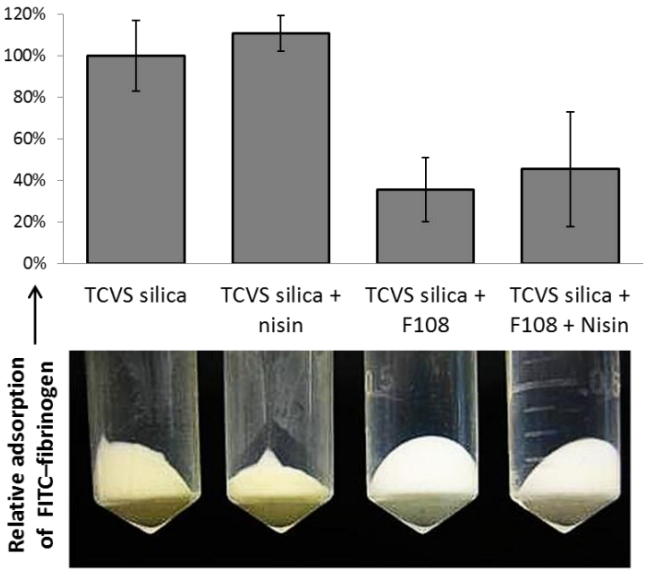

Figure 2.3: Relative adsorption of FITC-labeled fibrinogen onto hydrophobic TCVS and PEO-coated 1-µm silica microspheres. Measured absorbances and visible yellow tint indicate FITC-fibrinogen adsorption onto surfaces without PEO and insignificant difference between PEO-coatings with and without nisin.

2.3.2 Zeta potential of microsphere suspensions

As seen in Figure 2.4a, after consecutive fibrinogen challenges, F108 and F68-coated microspheres showed minimal change in zeta potential compared to their unchallenged counterparts. This result confirms the presence of a coating characteristic of one with sufficiently high chain density to form a brush layer. The small shift in zeta potential to a less negative value after fibrinogen contact observed with the F108 and F68 layers may be attributed to non-uniformities in the tri-block layer, giving rise to regions of unprotected hydrophobic silica that allow unhindered fibrinogen adsorption.

Consistent with results reported by Ryder *et al.*, a significant positive shift in zeta potential was recorded after nisin addition to F108 and F68 modified microspheres (Figure 2.4b) [1]. The smaller shift following nisin incubation for F68 surfaces compared to F108 surfaces indicates significantly less nisin loading in F68 layers as compared to F108 layers. From these results it was postulated that nisin becomes entrapped in both Pluronic® coatings, but to a lesser degree in F68 because of the shorter PEO chains.

Introduction of fibrinogen to both nisin-loaded triblock layers caused a decrease in zeta potential that was comparable to the decrease seen with consecutive buffer challenges (Figure 2.4b). Partial elution of nisin was observed with each buffer or fibrinogen challenge. These results suggest that nisin does not elute from the layers any faster when challenged with fibrinogen than with buffer and that nisin elution from tri-block coated surfaces may be independent of the presence of fibrinogen in solution.

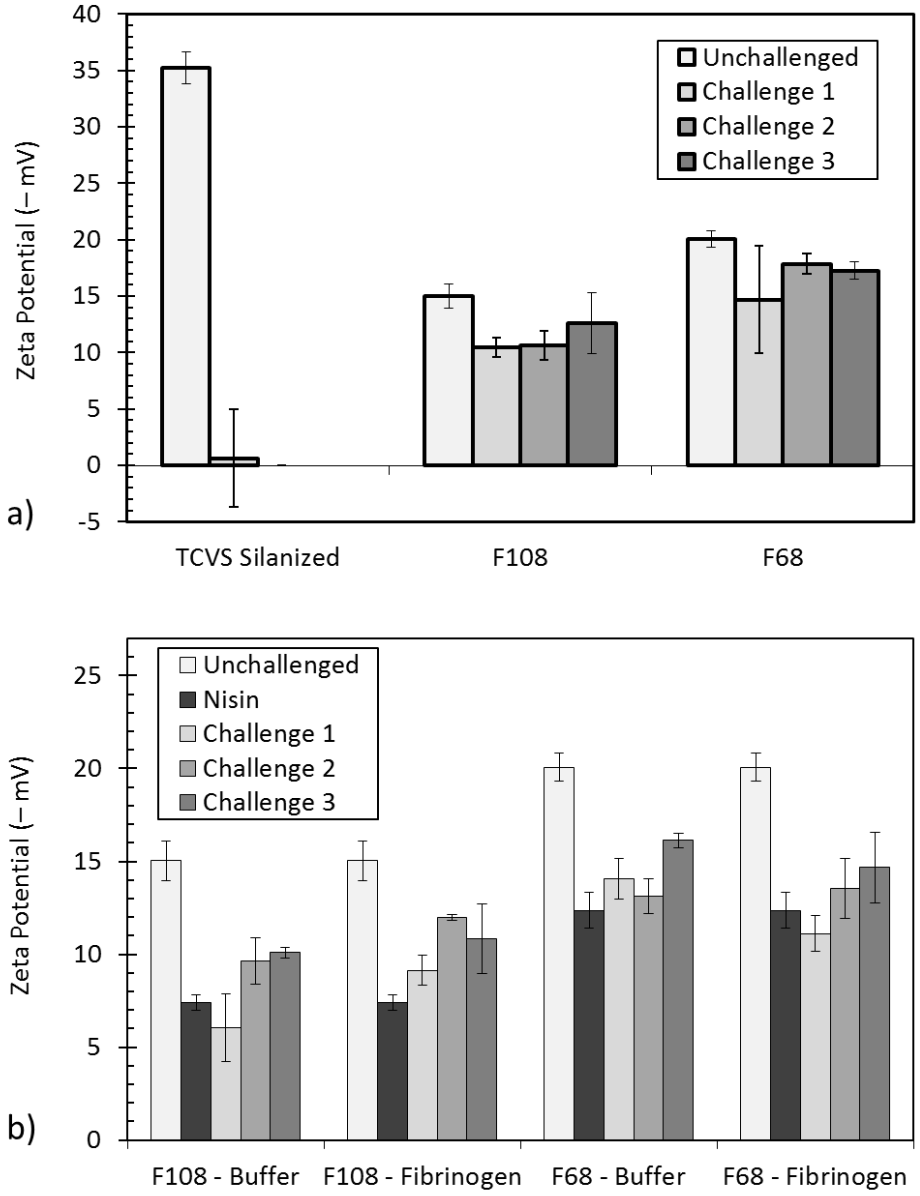

Figure 2.4: Zeta potential directly correlates to microsphere surface charge and so is indicative of molecules present at a surface. a) Zeta potential of F108 and F68 coated surfaces did not change significantly when challenged with fibrinogen. The layers were proved to be protein repelling. b) Zeta potential values for F108 and F68 coated surfaces increase with nisin introduction but marginally decrease with subsequent fibrinogen or buffer challenges. Notably there is no significant difference between the buffer and the fibrinogen challenges. Multiple protein adsorption/desorption scenarios may explain this observation.

2.3.3 Optical Waveguide Lightmode Spectroscopy (OWLS)

OWLS allows for direct detection of protein at a surface. Analysis of OWLS kinetic patterns provides great insight on the interfacial behavior of proteins at uncoated and coated surfaces. In a representative experiment, adsorption of nisin reached ~210 ng/cm^2 on a hydrophobic, TCVS-treated sensor then desorbed to approximately 190 ng/cm^2 upon rinsing with PBS (Figure 2.4a). In contrast, adsorption of nisin was decreased to ~100 ng/cm^2 on an F108-coated sensor, and desorbed to ~40 ng/cm^2 after rinsing with PBS. Nisin adsorption on an F68-coated sensor decreased even more to ~35 ng/cm^2 upon adsorption and ~10 ng/cm^2 after rinsing.

Fibrinogen adsorbed substantially onto uncoated, hydrophobic TCVS-treated sensors but not onto F108 and F68 coated sensors. Adsorption of fibrinogen on a TCVS-treated sensor previously exposed to nisin was less than a protein-free TCVS surface. The difference is likely due to decreased available surface area and competitive displacement or coverage of the adsorbed nisin by the much-larger fibrinogen, and is consistent with previous results of nisin/fibrinogen adsorption on uncoated polymer surfaces [1, 7]. Fibrinogen was not substantially desorbed from the uncoated sensors during rinsing. The slight increase in adsorbed mass during rinsing of the TCVS without nisin sensor was attributed to residual protein in the flow loop.

In contrast, OWLS sensors coated with γ-stabilized F108 or F68 brush layers exhibited markedly lower adsorption of fibrinogen (both less than 15 ng/cm^2), clearly demonstrating the repulsion of large proteins by the PEO brush (Figure 2.4b). Importantly, the presence of pre-adsorbed nisin in the brush had no effect on the adsorption of fibrinogen onto F108 and F68 coated sensors. The F108 and F68 PEO brush retained steric repulsive

activity against fibrinogen when loaded with nisin, despite the potential for electrostatic attraction between the two proteins.

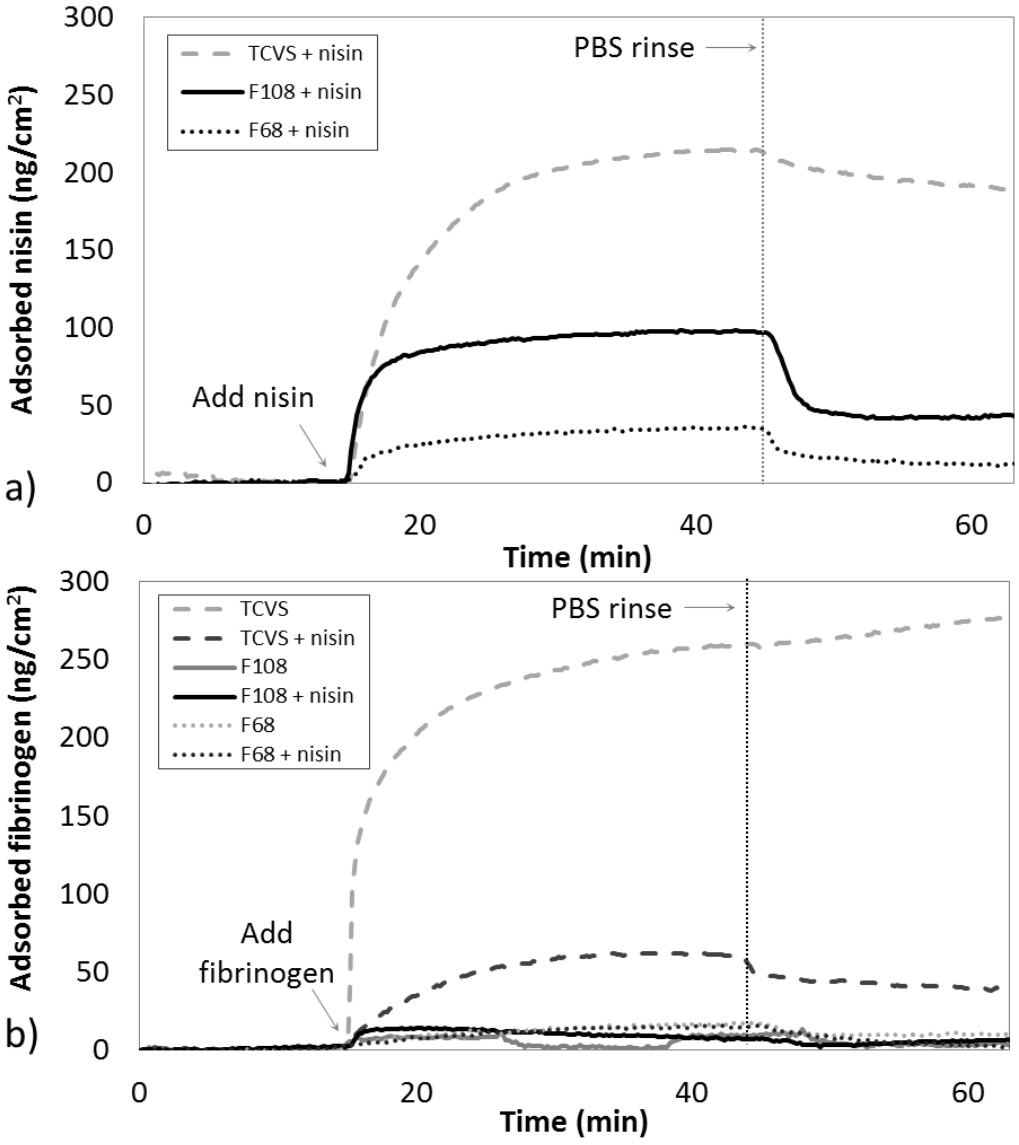

Figure 2.5: Adsorption and desorption of (a) nisin and (b) subsequent adsorption and desorption of fibrinogen onto hydrophobic TCVS or PEO-coated OWLS sensors.

Dill *et al*. used OWLS to record changes in adsorbed mass during cyclic adsorption-elution experiments with nisin, at uncoated and PEO-coated surfaces prepared with F108 or F68. Nisin adsorption was observed at uncoated and F108-coated surfaces in that work, but not at the F68-coated surfaces. Interpretation of the kinetic patterns recorded for uncoated and F108-coated surfaces with a history-dependent model of protein adsorption suggested nisin entrapment involved its location within the hydrophobic phase of the F108 brush, without contacting the underlying surface. While nisin entry into the F68 brush was observed during the adsorption step in that work, association with the surface and/or the surrounding PEO chains was not sufficient to show any measurable retention of the peptide during the rinse step. This complete elutability was suggested to be a result of the relatively short PEO chain length afforded by immobilized F68 being insufficient to form the level of attractive hydrophobic associations required for entrapment.

While Dill *et al*. recorded complete elution of nisin from the F68 brush upon introduction of protein-free buffer, the results reported here show a population of nisin, albeit small, that was resistant to elution at the F68 surface. The low fibrinogen adsorption observed at F68 layers with and without adsorbed nisin, while comparable to that recorded in similar experiments with F108 layers, is likely a result of there being only a small amount of nisin present at the F68 layer, presumably owing to its adsorption at (uncoated) defect regions on that surface. A small peptide capable of entrapment within a PEO brush layer would be expected to adsorb in significantly greater quantities than a larger protein that will be repelled by the PEO brush. Comparable adsorption of small and large peptides would be expected on uncoated spots on the surface. Figure 2.6 clearly shows that nisin adsorption to F108 was substantial in relation to any fibrinogen adsorption at that layer. On the other hand,

comparable adsorption of small (nisin) and large (fibrinogen) proteins recorded at the F68 layer is a fair expectation in the presence of uncoated regions on the surface.

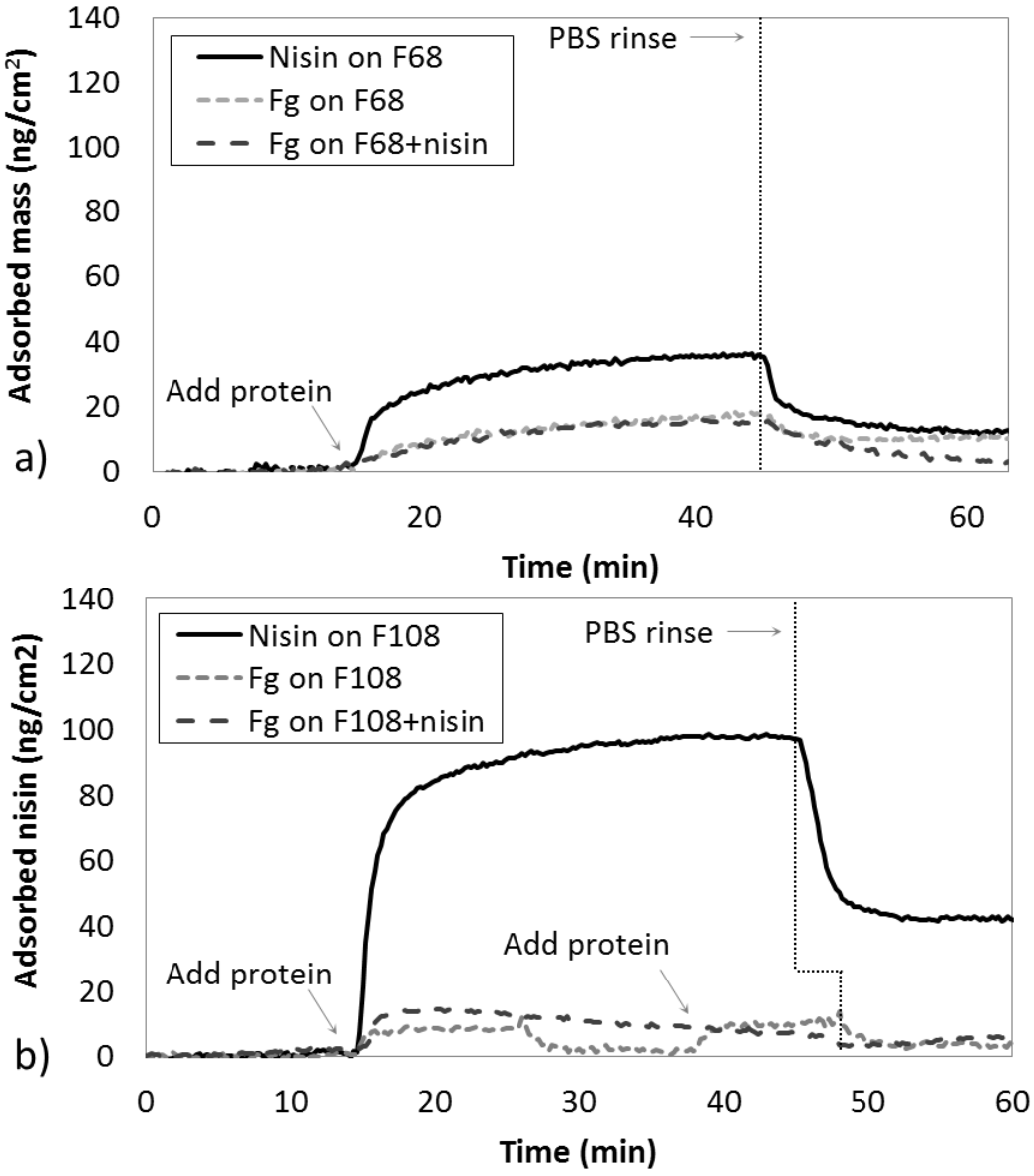

Figure 2.6: Fibrinogen adsorption on both F68 (a) and F108 (b) coatings was markedly low; however, nisin adsorption on the F68 coating was substantially lower than nisin adsorption on the F108 coating.

2.4 Conclusions

F108 and F68 coatings both exhibited considerable fibrinogen repulsion as compared to an uncoated, hydrophobic surface. However, nisin adsorption onto an F68 coated surface was clearly less than that onto an F108 coated surface. In fact, comparable nisin and fibrinogen adsorption onto an F68 coating indicates protein adsorption onto uncoated, defect regions. On the other hand, for an F108 coating nisin adsorption in amounts considerably greater than fibrinogen adsorption suggest nisin entrapment in the pendant PEO. The data presented supports the concept that an F108 coating has a sufficient inner hydrophobic region for complete entrapment such that PEO extends beyond the nisin and fibrinogen repulsion is retained.

2.5 Acknowledgments

This work was supported in part by the National Institute of Biomedical Imaging and Bioengineering (Grant No. R01EB011567). The content is solely the responsibility of the authors and does not necessarily represent the official views of NIBIB or the National Institutes of Health. The authors thank Ben Steyer, Alex Gerisimenko for providing zeta potential measurements.

2.6 References

[1] Ryder, M. P.; Schilke, K. F.; Auxier, J. A.; McGuire, J.; Neff, J. A., Nisin adsorption to polyethylene oxide layers and its resistance to elution in the presence of fibrinogen. *Journal of Colloid and Interface Science* **2010,** *350* (1), 194-199.

[2] Tai, Y. C.; Joshi, P.; McGuire, J.; Neff, J. A., Nisin adsorption to hydrophobic surfaces coated with the PEO-PPO-PEO triblock surfactant Pluronic (R) F108. *Journal of Colloid and Interface Science* **2008,** *322* (1), 112-118.

[3] Bosker, W. T. E.; Iakovlev, P. A.; Norde, W.; Stuart, M. A. C., BSA adsorption on bimodal PEO brushes. *Journal of Colloid and Interface Science* **2005,** *286*, 496-503.

[4] Norde, W.; Gage, D., Interaction of Bovine Serum Albumin and Human Blood Plasma with PEO-Tethered Surfaces: Influence of PEO Chain Length, Grafting Density, and Temperature. *Langmuir* **2004,** *20*, 4162-4167.

[5] Sofia, S. J.; Premnath, V.; W., M. E., Poly(ethylene oxide) Grafted to Silicon Surfaces: Grafting Density and Protein Adsorption. *Macromolecules* **1998,** *31*, 5059-5070.

[6] Huang, N.-P.; Michel, R.; Voros, J.; Textor, M.; Hofer, R.; Rossi, A.; Elbert, D. L.; Hubbell, J. A.; Spencer, N. D., Poly(L-lysine)-g-poly(ethylene glycol) Layers on Metal Oxide Surfaces: Surface-Analytical Characterization and Resistance to Serum and Fibrinogen Adsorption. *Langmuir* **2001,** *17*, 489-498.

[7] Tai, Y.-C.; McGuire, J.; Neff, J., Nisin antimicrobial activity and structural characteristics at hydrophobic surfaces coated wit the PEO-PPO-PEO triblock surfactant Pluronic® F108. *Journal of Colloid and Interface Science* **2008,** *322* (1), 104-111.

[8] Tseng, Y.-C.; McPherson, T.; Yuan, C. S.; Park, K., Grafting of ethylene glycol-butadiene block copolymers onto dimethyl-dichlorosilane-coated glass by γ-irradiation. *Biochemistry* **1995,** *16*.

[9] McPherson, T. B.; Shim, H. S.; Park, K., Grafting of PEO to glass, nitinol, and pyrolytic carbon surfaces by γ irradiation. *Journal of Biomedical Materials Research* **1997,** *38*.

[10] Unsworth, L. D.; Sheardown, H.; Brash, J. L., Protein-Resistant Poly(ethylene oxide)-Grafted surfaces: Chain Density-Dependent Multiple Mechanisms of Action. *Langmuir* **2008,** *24*, 1924-1929.

[11] Unsworth, L. D.; Sheardown, H.; Brash, J. L., Polyethylene oxide surfaces of variable chain density by chemisorption of PEO-thiol on gold: Adsorption of proteins from plasma studied by radiolabelling and immunoblotting. *Biomaterial* **2005,** *26* (30), 5927-5933.

[12] Higuchi, A.; Sugiyama, K.; Yoon, B. O.; Sakurai, M.; Hara, M.; Sumita, M.; Sugawara, S.-i.; Shirai, T., Serum protein adsorption and platelet adhesion on pluronic(TM)-adsorbed polysulfone membranes. *Biomaterials* **2003,** *24* (19), 3235-3245.

[13] Green, R. J.; Davies, M. C.; Roberts, C. J.; Tendler, S. J. B., A surface plasmon resonance study of albumin adsorption to PEO-PPO-PEO triblock copolymers. *Journal of Biomedical Material Research* **1998,** *42* (2), 165-171.

[14] Dill, J. K.; Auxier, J. A.; Schilke, K. F.; McGuire, J., Quantifying nisin adsorption behavior at pendant PEO layers. *Journal of Colloid and Interface Science* **2013**.

[15] Norde, W.; Giacomelli, C. E., BSA structural changes during homomolecular exchange between the adsorbed and the dissolved states. *Journal of Biotechnology* **2000,** *79*, 259-268.

[16] Wertz, C. F.; Santore, M. M., Fibrinogen Adsorption on Hydrophilic and Hydrophobic Surfaces: Geometrical and Energetic Aspects of Interfacial Relaxations. *Langmuir* **2002,** *18* (706-715).

[17] Tie, Y.; Ngankam, P.; Van Tassel, P. R., Probing Macromolecular Adsorbed Layer Structure and History Dependence via the Interfacial Cavity Function. *Langmuir* **2004,** *20*, 10599-10693.

[18] Breukink, E.; de Krujiff, B., Lipid II as a target for antibiotics. *Nature Reviews Drug Discovery* **2004,** *5*.

[19] Wiedemann, I.; Breukink, E.; van Kraaij, C.; Kuipersi, O. P.; Bierbaum, G.; de Krujiff, B.; Sahl, H.-G., Specific Binding of Nisin to the Peptidoglycan Precursor Lipid II Combines Pore Formation and Inhibition of Cell Wall Biosynthesis for Potent Antimicrobial Activity. *The Journal of biological Chemistry* **2001,** *276* (1), 1776-1779.

[20] Dreissen, A. J. M.; van den Hooven, H. W.; Kuiper, W.; van de Kamp, M.; Sahl, H.-G.; Koning, R. N. H.; Konings, W. N., Mechanistic studies of lantibiotic-induced permeabilization of phospholipid vesicles. *Biochemistry* **1995,** *34*, 1606-1614.

[21] Ruhr, E.; Sahl, H.-G., Mode of action of the peptide antibiotic nisin and influence of the membrane potential of whole cells and on cytoplasmic and artificial membrane vesicles. *Antimicrobial Agents and Chemotherapy* **1985,** *27*, 841-845.

[22] Hsu, S.-T.; Breukink, E.; Tischenki, E.; Lutters, M. A. G.; de Kruijiff, B.; Kaptein, R.; Bonvin, A. M. J.; van Nuland, N. J., The nisin-lipid II complex reveals a pyrophosphate cage that provides a blueprint for novel antibiotics. *Nature Structural & Molecular Biology* **2004,** *11* (10).

[23] Halperin, A., Polymer brushes that resist adsorption of model proteins: Design parameters. *Langmuir* **1999,** *15*.

[24] Schilke, K. F.; McGuire, J., Detection of nisin and fibrinogen adsorption on poly (ethylene oxide) coated polyurethane surfaces by time-of-flight secondary ion mass spectrometry (TOF-SIMS). *Journal of colloid and interface science* **2011**.

[25] Salmio, H.; Bruhwiler, D., Distribution of amino groups on a mesoporous silica surface after submonolayer deposition of aminopropylsilanes from an anhydrous liquid phase. *Journal of Physical Chemistry* **2007,** *C111*.

[26] Székács, A.; Adányi, N.; Székács, I.; Majer-Baranyi, K.; Szendrö, I., Optical waveguide light-mode spectroscopy immunosensors for environmental monitoring. *Applied Optics* **2009,** *48* (4), B151-B159.

ACTIVITY RETENTION OF NISIN ENTRAPPED IN PENDANT PEO BRUSH COATINGS

Julie A. Auxier, Karl F. Schilke, Joe McGuire

School of Chemical, Biological and Environmental Engineering, Oregon State University, Corvallis, OR 97331

*Corresponding author:

Gleeson Hall Rm. 102
Oregon State University
Corvallis, OR 97331 USA
E-mail: *joseph.mcguire@oregonstate.edu*
Telephone: 1-541-737-6306
Fax: 1-541-737-4600

CHAPTER 3

ACTIVITY RETENTION OF NISIN ENTRAPPED IN PENDANT PEO BRUSH COATINGS

Abstract

Nisin, a small cationic, amphiphilic peptide is an effective inhibitor of Gram-positive bacteria whose mode of action does not encourage pathogenic resistance. Its potential use in anti-infective coating strategies has motivated interest in its adsorption and function at biomaterial interfaces. Nisin adsorption and various aspects of its behavior at poly(ethylene oxide) (PEO) coated surfaces have been described through surface characterization techniques and shown that the protein repelling capacity of a PEO layer following nisin entrapment is retained. It therefore was expected that the immobilized, pendant PEO chains will inhibit exchange of entrapped nisin by competing proteins, and therefore prolong nisin activity retention. In order to evaluate nisin function following its entrapment, the antimicrobial activity of nisin-loaded, F108-coated silica surfaces was evaluated against the Gram-positive indicator strain, *Pediococcus pentosaceous*. The retained biological activity of these nisin-loaded layers was evaluated after incubation in the presence of bovine serum albumin (BSA), for contact periods up to one week. Surfaces were withdrawn at selected times and placed on plates inoculated with *P. pentosaceous* to measure kill zone radius in order to quantify nisin activity. In the presence of BSA, F108-coated surfaces retained more antimicrobial activity than the uncoated, hydrophobic surfaces. These results strongly suggest that PEO brush layers may serve as a viable drug storage platform due to the retained non-fouling character after bioactive peptide entrapment and the prolonged peptide activity in the presence of other proteins.

3.1 Introduction

Nisin is a popular bacteriocin approved for use as a food preservative in over forty countries [1]. It is a naturally occurring, amphiphilic peptide from *Lactococcus lactis* whose mode of action does not encourage pathogenic resistance [1]. Nisin inactivates Gram-positive bacteria by pore formation in cellular membranes. Nisin molecules attach to lipid II, a precursor of cell wall synthesis, form a cage-like structure, and destroy transmembrane potential and pH gradient causing cellular material to exit the cell [1-3]. Attachment to lipid II results in highly specific pores and nisin activity in nanomolar quantities [2].

Food contamination by microbes results in accelerated spoilage and foodborne illness [4] and was recently observed in a salmonella outbreak in a New Mexico nut butter plant that contaminated peanut butter products, causing a number of nationwide salmonella cases [5]. Incorporation of antimicrobials in food packaging would reduce the risk of contamination and also enhance food shelf-life, stability, and quality [6]. Bioactive packaging could prevent spoilage at the surface [6] and provide increased product safety [4].

Nisin has been extensively studied and reviewed [1,7,8]. It has been considered for and studied in food packaging where the packaging directly contacts the product and food contacting surfaces [6]. Nisin is not volatile and requires direct contact for diffusion to the target product.

Physiochemical environmental factors greatly influence the activity of nisin including pH, temperature, food matrix composition, and enzymatic activity [1,9]. Nisin is more active in lower pH environments and so applications to higher surface pH, such as in meat, may be less effective [1]. A minimum inhibitory concentration (MIC) must be maintained at the package-food interface for effectiveness [6]. Factors compromising nisin concentration or activity at surface-food interface may decrease available nisin below the threshold

concentration. Direct application of nisin quickly loses activity due to displacement by food matrix proteins, rapid diffusion from the surface, or inactivation by product constituents [4]. Therefore, the delivery mechanism of nisin to the product must protect activity and control diffusion from the surface.

Nisin has been previously shown to be an effective antimicrobial in packaging coatings [10]. Delivery mechanisms to preserve nisin activity in food systems that have been investigated include liposomes, polymers as film coatings, microencapsulation, and nanoparticles [9,11]. Nisin loaded on liposomal nanoparticles was shown to extend activity against *L. monocytogenes* and *S. aureus* as compared to free nisin [9]. Nisin-coated film has also been shown to inhibit *M. luteus* growth, though kinetics were unpredictable [12]. A study of release kinetics of nisin from polyethylene/olyamide/polyethylene film indicated increasing salt concentration and temperature, but not pH, decreased desorption rates [11]. A study of nisin release from homogenized solid lipid nanoparticles showed prolonged nisin activity over 15-20 days as compared to free nisin (3 days) and described that increases in pH and salt concentration decreased the release rate [13]. The authors noted low efficiencies for nisin encapsulation in solid lipid nanoparticles and a preference for nisin to adsorb to the surface, likely due to the high hydrophobicity of the lipid [13]. Incorporation of nisin into PLA also demonstrated increased activity retention against *L. monocytogenes*, *E. coli*, and *S. Enteritidis* as compared to free nisin [14,15].

The aforementioned methods adequately deliver nisin to the target product, but they do not address concerns around protein interactions at the surface of the coatings or particles. It can be expected that some proteins in the food matrix will preferentially associate to interfaces depending on the matrix composition and protein hydrophobicities [16]. Protein adsorption to a coating may displace or inactivate nisin, thereby reducing the coating

efficiency. Previous work has shown that nisin becomes entrapped in Pluronic® F108, pendant polyethylene oxide (PEO) brush layers such that nisin does not associate with the surface, but also has PEO extending beyond it into the bulk [17-19]. The presence of nisin in the PEO brush does not encourage protein adsorption any more than a brush layer without nisin and extensive work has been conducted on the interfacial mechanisms and kinetics of nisin and fibrinogen adsorption at PEO brush layers [17-19].

The PEO protects the entrapped nisin from bulk proteins, but does not prevent concentration gradient driven diffusion of nisin from the coating. Nisin adsorbed directly on a surface is subject to denaturation, displacement by bulk proteins, and rapid diffusion from the surface (Figure 3.1). Therefore, the protective PEO could be expected to extend the activity of nisin entrapped PEO in comparison to adsorbed nisin. The work presented here sought to demonstrate retained activity of antimicrobial agents entrapped in pendant PEO while retaining PEO's protein repulsive character in a model protein matrix.

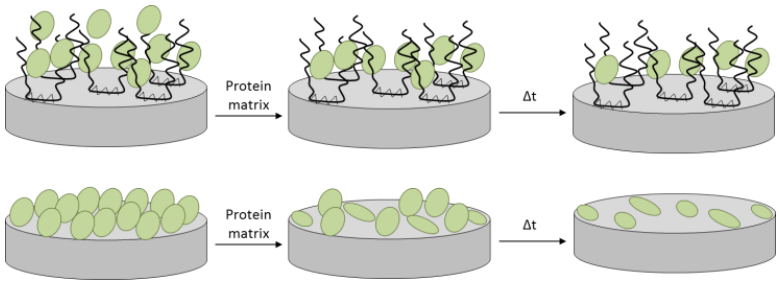

Figure 3.1: Nisin becomes entrapped in F108 layers. Upon contact with protein solution, outer nisin will more readily elute from the layer than inner nisin. The PEO extending beyond entrapped nisin will retain repulsive character and protect the nisin so that nisin may diffuse into solution over time, resulting in retained activity. Conversely, nisin adsorbs to hydrophobic surfaces in multilayer quantities that easily denature or are displaced upon contact with protein solution. Over time remaining nisin will lose activity.

3.2 Materials and methods

3.2.1 Surface modifications and PEO coatings

Silica wafers (1 cm^2, WaferNet, San Jose, CA) were RCA cleaned using 5 H_2O: 5 NaOH: 1 H_2O_2 for 10 min at 80 °C followed by 5 H_2O: 5 HCl: 1 H_2O_2 for 10 min at 80 °C. SiO_2-coated sensors for optical waveguide lightmode spectroscopy (OWLS 210, MicroVacuum, Budapest, Hungary) were cleaned using chromosulphuric acid. OWLS sensors and wafers were then silanized at 25 °C with trichlorovinylsilane (TCVS) vapor and cured for 30 min at 120 °C. TCVS-modified surfaces were coated by adsorption of 10 mg/mL Pluronic® F108 triblocks in 10 mM sodium phosphate buffer with 150 mM NaCl, pH 7.4 (PBS) [19-20]. The adsorbed PEO brush was covalently stabilized by γ-irradiation (^{60}Co, 0.3 Mrad) [22].

3.2.2 Solution preparations

Nisin solution (3.4 kDa, 0.5 mg/mL, Prime Pharma, Gordons Bay, South Africa) was prepared in PBS and filtered (0.2 μm) immediately before use. Frozen equine plasma (HemoStat Laboratories, Inc.) was thawed and diluted to 25% v/v with PBS immediately before use. Bovine serum albumin (BSA) solution (~66 kDa, 1 mg/mL, Sigma-Aldrich) was prepared in 20 mM phos-citrate buffer, pH 4.0, and filtered (0.2 μm) as needed.

3.2.3 OWLS

OWLS provides real time detection of protein adsorption on sensors without labeling. Sensors with and without γ-stabilized F108 were equilibrated in PBS overnight. After a steady baseline was achieved, freshly made 0.5 mg/mL nisin in PBS was injected into the flow loop and passed over the sensor (50 μL/min) for 30 min then rinsed with PBS for 30 min as appropriate. Subsequently, 25% equine plasma in PBS was injected, passed over the sensor for

30 min, and then rinsed with PBS for 30 min. The plasma injection cycle was repeated. Plasma was also added to a TCVS-modified sensor for comparison.

3.2.4 Bacterial preparation

Pediococcus pentosaceus was cultured overnight at 37 °C in sterile MRS broth (52.2 g/L). Sterile MRS agar plates (1% agar, Difco) were inoculated with approximately 10^5 CFU/mL of *P. pentosaceus*. Plates were freshly made for each sampling.

3.2.5 Minimum inhibitory concentration

Serial dilutions of nisin (starting at 0.5 mg/mL, dilution factors 10^0-10^4) in PBS at pH 7.0 and 20 mM phosphate-citrate buffer at pH 4.0 were prepared in a 96 well plate (50 µL). 50 µL of *P. pentosaceus* overnight culture and 100 µL of sterile MRS broth were added to each well and incubated at 37 °C overnight. Turbidity was measured at 280 nm.

3.2.6 Activity assay

Modified silica wafers were placed individually in wells of a 24-well plate to which 1 mL BSA solution was added (enough to cover wafer). All wafers in well plates were placed on an orbital shaker at 37 °C for the duration of the assay.

Select wafers were removed from wells, excess solution removed from surface and placed inverted on *P. pentosaceus* inoculated plates. Bacterial plates were incubated at 37 °C for 48 h after which bacterial kill zones, defined as the distances of the halo from the wafer edge, were measured and photographed. All samplings were performed in triplicate.

3.3 Results and Discussion

3.3.1 OWLS

Diluted equine plasma adsorbed to a hydrophobic TCVS surface to a maximum of ~290 ng/cm^2 and rinsed to ~215 ng/cm^2. In contrast, diluted plasma adsorbed to an F108 coated surface to ~165 ng/cm^2 and rinsed to ~85 ng/cm^2. The F108 coating clearly imparted some degree of protein repelling function to the surface. The observed adsorption on the F108 layer may be attributed to imperfections in the coating or small peptide components of the plasma integrating into the PEO brush. The presence of nisin in an F108 layer resulted in diluted plasma adsorption to a maximum of ~140 ng/cm^2 and rinsed to ~70 ng/cm^2. The equine plasma adsorbed to F108 coated OWLS sensors with and without nisin in approximately equal amounts; both substantially lower than adsorption to TCVS (Figure 3.2).

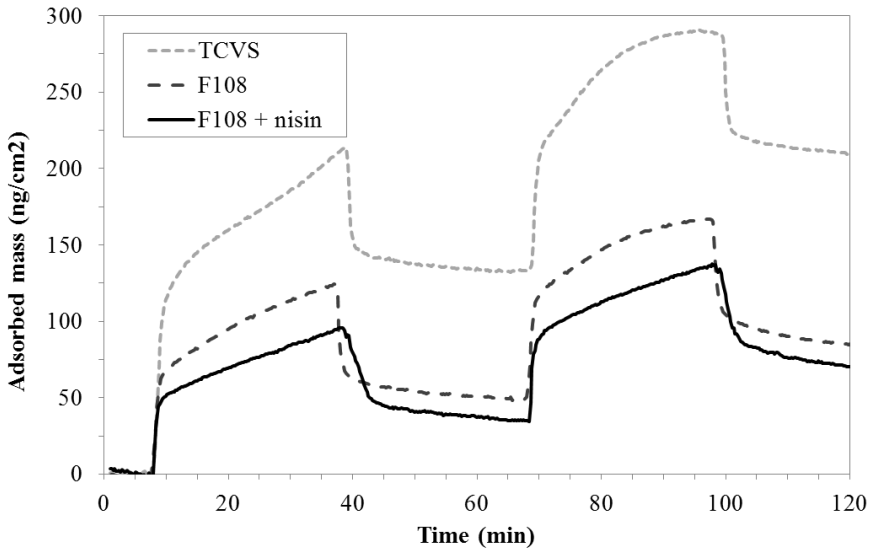

Figure 3.2: OWLS measurements were collected as equine plasma diluted to 25% in PBS was cyclically contacted and rinsed on hydrophobic TCVS and F108 coated (with and without nisin) OWLS sensors. Plasma adsorbed to a greater degree on the TCVS surface compared to F108 surfaces. Plasma adsorbed in approximately equal amounts to F108 sensors with and without nisin.

Previous work with nisin entrapment in PEO has investigated single protein challenges, never whole plasma. The results with plasma are comparable to past OWLS tests involving fibrinogen, a large blood protein (340 kDa), adsorption to PEO coatings with entrapped nisin [17-18]. For comparison, OWLS results for BSA, a smaller blood protein (66 kDa), adsorption to F108 surfaces with and without nisin (data not shown) indicated protein adsorption at the surface consistent with the dilute plasma results. The results of these plasma challenges are encouraging for complex protein matrix applications.

3.3.2 Minimum inhibitory concentration

The minimum inhibitory concentration (MIC) of nisin in two buffer systems was conducted to determine the extent of nisin activity in the different pH environments and validate buffer choice in the activity assay. The MIC for nisin in phosphate-citrate buffer at pH 4.0 was measured to be 15.6 μg/mL (4.6 nmol/mL). The MIC for nisin in PBS at pH 7.0 was measured to be 62.5 μg/mL (18.4 nmol/mL). The stark difference between the two activities was expected based on previous work with nisin activity dependence on pH [1,9,13]. Based on these results, the model surfaces in the activity assay were incubated in model protein solution at pH 4.0 to allow higher nisin activity and easier detection of retained activity.

3.3.3 Activity assay

The similarity between single protein and whole plasma challenges with OWLS suggests that nisin activity retention will also be comparable for single protein and whole plasma challenges in so far as to prove the proposed activity retention mechanism. Therefore, BSA was chosen as a model protein matrix. BSA was chosen because its adsorption to PEO brushes has been studied and quantified [23-27]. BSA would be expected to interact with the

PEO due to hydrophilic attraction [24,26,27] and so adequately serve as a simple model matrix.

Representative kill zone radii for the two surfaces, nisin adsorbed onto hydrophobic TCVS modified silica (TCVS) and nisin entrapped F108 coated silica (F108), are presented in Figure 3.3. On day zero, both surfaces showed similar activity before challenged with BSA solution. Upon challenge with the BSA solution, the surface adsorbed nisin quickly lost activity as evidenced by the rapid decrease in kill zone. The nisin entrapped in F108, however, retained activity to a larger degree than the surface adsorbed nisin for the seven days examined, as seen by the larger kill zone (Figure 3.3).

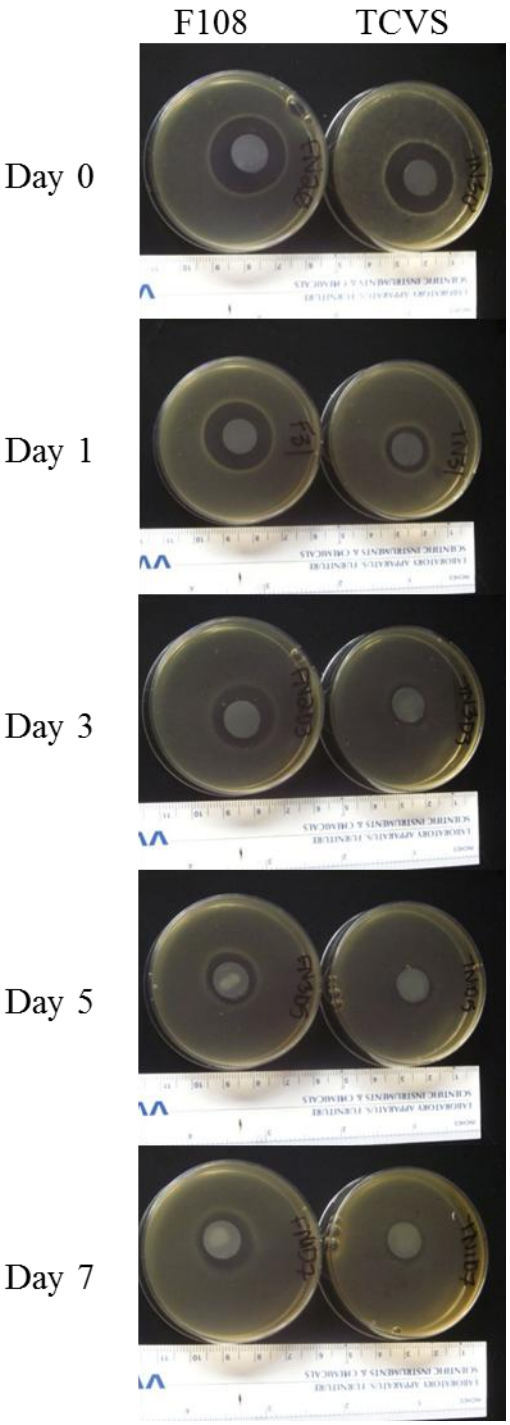

Figure 3.3: Silica wafers modified with nisin entrapped in F108 (F108) or surface adsorbed nisin (TCVS) were challenged with BSA solution (pH 4.0) and plated against *P. pentosaceus* to quantify nisin activity over time. Surface adsorbed nisin kill zones decreased rapidly, indicating rapid activity loss. Entrapped nisin kill zones were more pronounced for longer, suggesting that entrapment in F108 allows for activity retention.

Initially, the slightly greater activity of surface adsorbed nisin compared to the entrapped nisin may be attributed to multilayer quantities of nisin initially available at the surface. After exposure to BSA, an exponential decrease in activity was seen for both surfaces; however, the initial decrease of surface adsorbed nisin activity was significantly greater than the decrease of F108 entrapped nisin activity. The significant differences in kill zone became more pronounced as time passed. The entrapped nisin seemed to plateau by Day 7, whereas the surface adsorbed nisin continued to decrease to negligible activity (Figure 3.4). Had the experiment run longer, sustained nisin activity in the PEO could have been expected. The activity of nisin entrapped in F108 on Day 7 was approximately equal to the activity observed for TCVS surface adsorbed nisin on Day 1. It may be concluded that nisin entrapment in F108 increases activity retention over time when exposed to surface attracted proteins.

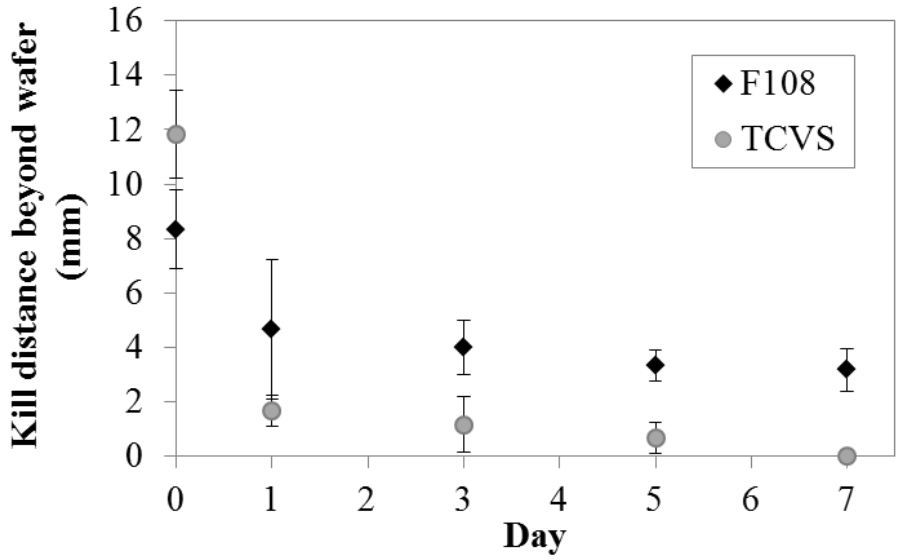

Figure 3.4: Average kill zones, measured as the distance of halo extending beyond the perimeter of the wafer, of “F108” and “TCVS” surfaces over time indicate significant differences between the two surface activities. Both exhibit initial exponential activity loss. Nisin in F108 activity plateaus by Day 7 whereas nisin on TCVS becomes negligible by Day 7.

The rapid decrease of surface adsorbed nisin activity suggests denaturation or competitive displacement upon contact with surface active protein. The initial activity decrease of entrapped nisin is consistent with outer nisin eluting from surface more quickly than inner nisin. The observed plateau region of entrapped nisin activity suggests nisin elute from the PEO by controlled diffusion. These observations are consistent with the proposed mechanism (Figure 3.1).

Nisin is an ideal candidate for antimicrobial applications to food system protection, namely in bioactive food packaging or food contacting surface coatings. Additionally, there are potential medical applications for peptide entrapment in PEO; however, nisin would likely be replaced by another, more clinically applicable amphiphilic peptide. Nisin entrapment in F108 layers showed retained activity greater and for longer time than nisin adsorbed to a hydrophobic surface. The retained nisin activity, in combination with retained PEO protein repulsive character make this system and mechanism a promising method for applications in food processing and packaging protection and safety.

3.4 Acknowledgements

This work was supported in part by the National Institutes of Biomedical Imaging and Bioengineering (NIBIB, grant no. R01EB011567). The authors would like to thank Tom Shellhammer for use of lab equipment during activity assay testing in addition to Justen Dill, Josh Snider, and Lars Bowlin for additional laboratory assistance.

3.5 References

[1] Cleveland, J.; Monteville, T. J.; Nes, I. F.; Chikindas, M. L., Bacteriocins: safe, natural antimicrobials for food preservation. *International Journal of Food Microbiology* **2001,** *71* (1), 1-20.

[2] Wiedemann, I.; Breukink, E.; van Kraaij, C.; Kuipersi, O. P.; Bierbaum, G.; de Krujiff, B.; Sahl, H.-G., Specific Binding of Nisin to the Peptidoglycan Precursor Lipid II Combines Pore Formation and Inhibition of Cell Wall Biosynthesis for Potent Antimicrobial Activity. *The Journal of biological Chemistry* **2001,** *276* (1), 1776-1779.

[3] Hsu, S.-T.; Breukink, E.; Tischenki, E.; Lutters, M. A. G.; de Kruijiff, B.; Kaptein, R.; Bonvin, A. M. J.; van Nuland, N. J., The nisin-lipid II complex reveals a pyrophosphate cage that provides a blueprint for novel antibiotics. *Nature Structural & Molecular Biology* **2004,** *11* (10).

[4] Quintavalla, S.; Vicini, L., Antimicrobial food packaging in meat industry. *Meat Science* **2002,** *62*, 373-380.

[5] Jalonick, M. C., Salmonella confirmed in peanut butter plant. *Associated Press* October 5, 2012.

[6] Appenini, P.; Hotchkiss, J. H., Review of antimicrobial food packaging. *Innovative Food Science & Emerging Technologies* **2002,** *3*, 113-126.

[7] Abee, T., Pore-forming bacteriocins of Gram-positive bacteria and self-protection mechanisms of producer organisms. *FEMS Microbiology Letters* **1995,** *129* (1), 1-9.

[8] Delves-Broughton, J.; Blackburn, P.; Evans, R.; Hugenholtz, J., Applications of the bacteriocin, nisin. *Antonie van Leeuwenhoek* **1996,** *69* (2), 193-202.

[9] Zou, Y.; Lee, H.-Y.; Seo, Y.-C.; Ahn, J., Enhanced antimicrobial activity of nisin-loaded liposomal nanoparticles against foodborne pathogens. *Journal of Food Science* **2012,** *77* (3).

[10] Cooksey, K., Effectiveness of antimicrobial food packaging materials. *Food Additives and Contamination* **2005,** *22* (10), 980-987.

[11] Guiga, W.; Galland, S.; Peyrol, E.; Degraeve, P.; Carnet-Pantiez, A.; Sebti, I., Antimicrobial plastic film: Physico-chemical characterization and nisin desorption modeling. *Innovative Food Science & Emerging Technologies* **2009,** *10* (2), 203-207.

[12] Mauriello, G.; De Luca, E.; La Storia, A.; Vallani, F.; Ecrolini, D., Antimicrobial activity of a nisin-activated plastic film for food packaging. *Letters in Applied Microbiology* **2005,** *41*, 464-469.

[13] Prombutara, P.; Kulwatthanasal, Y.; Spaka, N.; Sramala, I.; Chareonpornwattana, S., Production of nisin-loaded solid lipid nanoparticles for sustained antimicrobial activity. *Food Control* **2002,** *24*, 184-190.

[14] Jin, T.; Zhang, H., Biodegradable Polylactic Acid Polymer with Nisin for Use in Antimicrobial Food Packaging. *Food Microbiology and Safety* **2008,** *73* (9).

[15] Salmaso, S.; Elvassore, N.; Bertucco, A.; Lante, A.; Caliceti, P., Nisin-loaded poly-l-lactide nano-particles produced by CO2 anti-solven$_t$ precipitation for sustained antimicrobial activity. *International Journal of Pharmaceutics* **2004,** *287* (1-2), 163-173.

[16] Damodaran, S.; Fennema, O.; Parkin, K., *Food Chemistry*. 4th ed.; CRC Press: 2007.

[17] Tai, Y. C.; Joshi, P.; McGuire, J.; Neff, J. A., Nisin adsorption to hydrophobic surfaces coated with the PEO-PPO-PEO triblock surfactant Pluronic (R) F108. *Journal of Colloid and Interface Science* **2008,** *322* (1), 112-118.

[18] Tai, Y.-C.; McGuire, J.; Neff, J., Nisin antimicrobial activity and structural characteristics at hydrophobic surfaces coated wit the PEO-PPO-PEO triblock surfactant Pluronic® F108. *Journal of Colloid and Interface Science* **2008,** *322* (1), 104-111.

[19] Ryder, M. P.; Schilke, K. F.; Auxier, J. A.; McGuire, J.; Neff, J. A., Nisin adsorption to polyethylene oxide layers and its resistance to elution in the presence of fibrinogen. *Journal of Colloid and Interface Science* **2010,** *350* (1), 194-199.

[20] Popat, K. C.; Johnson, R. W.; Desai, T. A., Characterization of vapor deposited thin silane film on silicon substrates for biomedical microdevices. *Surface and Coatings Technology* **2002,** *154*, 253-261.

[21] Popat, K. C.; Sadhana, S.; Johnson, R. W.; Desai, T. A., AFM analysis of organic silane thing films for bioMEMS applications. *Surface and Interface Analysis* **2003,** *35*, 205-215.

[22] McPherson, T. B.; Shim, H. S.; Park, K., Grafting of PEO to glass, nitinol, and pyrolytic carbon surfaces by γ irradiation. *Journal of Biomedical Materials Research* **1997,** *38*.

[23] Kiss, E.; Dravetzky, K.; Hill, K.; Kutnyanszky, E.; A., V., Protein interaction with a Pluronic-modified poly9lactic acid) Langmuir monolayer. *Journal of colloid and Interface Science* **2008**.

[24] Norde, W.; Gage, D., Interaction of Bovine Serum Albumin and Human Blood Plasma with PEO-Tethered Surfaces: Influence of PEO Chain Length, Grafting Density, and Temperature. *Langmuir* **2004,** *20*, 4162-4167.

[25] Sofia, S. J.; Premnath, V.; W., M. E., Poly(ethylene oxide) Grafted to Silicon Surfaces: Grafting Density and Protein Adsorption. *Macromolecules* **1998,** *31*, 5059-5070.

[26] Jeyachandran, Y. L.; Mielczarski, E.; Rai, B.; Mielczarski, J. A., Quantitative and Qualitative Evaluation of Adsorption/Desorption of Bovine Serum Albumin on Hydrophilic and Hydrophobic Surfaces. *Langmuir* **2009,** *25* (19), 11614-11620.

[27] Bosker, W. T. E.; Iakovlev, P. A.; Norde, W.; Stuart, M. A. C., BSA adsorption on bimodal PEO brushes. *Journal of Colloid and Interface Science* **2005,** *286*, 496-503.

CHAPTER 4

GENERAL CONCLUSIONS

The work presented here offers insight on the viability of bioactive PEO brush coatings for biomaterial applications. It offers a complete picture of the effectiveness of each component of the coating. The effects of nisin integration into PEO brush on the brush protein repulsion ability in addition to the effects of PEO brush on nisin activity retention in a model system were investigated.

Pluronic® PEO brush layers were successfully grafted onto hydrophobic silica surfaces. These model surfaces were challenged with the large protein fibrinogen and relatively the small peptide nisin. Protein adsorption was quantified with a number of analytical methods. Results from these challenges shed light on the protein repelling capabilities of a PEO brush before and after nisin entrapment, and demonstrated that nisin becomes entrapped in Pluronic® F108 brush layers but not in F68 brush layers. F108 contains a hydrophobic inner region sufficient for substantial nisin entrapment while still remaining protein repellant. Although F68 does repel protein after exposure to nisin, it does not adsorb nisin consistent with entrapment. This proof lends credibility to using a PEO brush as a drug reservoir.

Furthermore, F108 brush layers with and without nisin were challenged with diluted equine plasma. Plasma protein adsorption was similar for these surfaces and the magnitudes of both were less than that of a surface without a PEO brush coating. The results of these plasma challenges are encouraging for complex protein matrix applications. Activity of nisin entrapped in F108 and challenged with BSA in comparison with surface adsorbed nisin challenged with BSA was quantified over a week long period. Nisin activity when entrapped

in F108 brush layers was shown to retain activity significantly longer than surface bound nisin against *P. pentosaceus*. This work successfully proved the concept of enhanced nisin activity retention upon entrapment in PEO brush layers containing an adequate hydrophobic inner region.

Knowledge gained of this model system is valuable for future applications of bioactive peptide integration to surfaces contacting a protein matrix. Nisin is applicable for some food systems, but is less attractive for clinical applications. Entrapment of a peptide more effective against clinically relevant bacteria should be investigated. This work successfully characterized the important interacting factors of a model drug delivery system. Conclusions drawn from the work support further examination and application of peptide entrapment in PEO brush layers with sufficient hydrophobic inner regions as bioactive coatings for protein contacting interfaces in biotechnology.

CHAPTER 5

BIBLIOGRAPHY

Abee, T., Pore-forming bacteriocins of Gram-positive bacteria and self-protection mechanisms of producer organisms. *FEMS Microbiology Letters* **1995,** *129* (1), 1-9.

Appenini, P.; Hotchkiss, J. H., Review of antimicrobial food packaging. *Innovative Food Science & Emerging Technologies* **2002,** *3*, 113-126.

Bosker, W. T. E.; Iakovlev, P. A.; Norde, W.; Stuart, M. A. C., BSA adsorption on bimodal PEO brushes. *Journal of Colloid and Interface Science* **2005,** *286*, 496-503.

Bower, C. K.; Bothwell, M. K.; McGuire, J., Lantibiotics as surface active agents for biomedical applications. *Colloids and Surface B: Biointerfaces* **2001,** *22* (4), 259-265.

Bower, C. K.; Parker, J. E.; Higgins, A. Z.; Oest, M. E.; Wilson, J. T.; Valentine, B. A.; Bothwell, M. K.; McGuire, J., Protein antimicrobial barriers to bacterial adhesion: in vitro and in vivo evaluation of nisin-treated implantable materials. *Colloids and Interfaces B: Biointerfaces* **2002,** *25* (1), 81-90.

Breukink, E.; de Krujiff, B., Lipid II as a target for antibiotics. *Nature Reviews Drug Discovery* **2004,** *5*.

Cleveland, J.; Monteville, T. J.; Nes, I. F.; Chikindas, M. L., Bacteriocins: safe, natural antimicrobials for food preservation. *International Journal of Food Microbiology* **2001,** *71* (1), 1-20.

Cooksey, K., Effectiveness of antimicrobial food packaging materials. *Food Additives and Contamination* **2005,** *22* (10), 980-987.

Damodaran, S.; Fennema, O.; Parkin, K., *Food Chemistry*. 4th ed.; CRC Press: 2007.

Delves-Broughton, J.; Blackburn, P.; Evans, R.; Hugenholtz, J., Applications of the bacteriocin, nisin. *Antonie van Leeuwenhoek* **1996,** *69* (2), 193-202.

Dill, J. K.; Auxier, J. A.; Schilke, K. F.; McGuire, J., Quantifying nisin adsorption behavior at pendant PEO layers. *Journal of Colloid and Interface Science* **2013**.

Dreissen, A. J. M.; van den Hooven, H. W.; Kuiper, W.; van de Kamp, M.; Sahl, H.-G.; Koning, R. N. H.; Konings, W. N., Mechanistic studies of lantibiotic-induced permeabilization of phospholipid vesicles. *Biochemistry* **1995,** *34*, 1606-1614.

Green, R. J.; Davies, M. C.; Roberts, C. J.; Tendler, S. J. B., A surface plasmon resonance study of albumin adsorption to PEO-PPO-PEO triblock copolymers. *Journal of Biomedical Material Research* **1998,** *42* (2), 165-171.

Guiga, W.; Galland, S.; Peyrol, E.; Degraeve, P.; Carnet-Pantiez, A.; Sebti, I., Antimicrobial plastic film: Physico-chemical characterization and nisin desorption modeling. *Innovative Food Science & Emerging Technologies* **2009,** *10* (2), 203-207.

Halperin, A., Polymer brushes that resist adsorption of model proteins: Design parameters. *Langmuir* **1999,** *15*.

Higuchi, A.; Sugiyama, K.; Yoon, B. O.; Sakurai, M.; Hara, M.; Sumita, M.; Sugawara, S.-i.; Shirai, T., Serum protein adsorption and platelet adhesion on pluronic(TM)-adsorbed polysulfone membranes. *Biomaterials* **2003,** *24* (19), 3235-3245.

Hsu, S.-T.; Breukink, E.; Tischenki, E.; Lutters, M. A. G.; de Kruijiff, B.; Kaptein, R.; Bonvin, A. M. J.; van Nuland, N. J., The nisin-lipid II complex reveals a pyrophosphate cage that provides a blueprint for novel antibiotics. *Nature Structural & Molecular Biology* **2004,** *11* (10).

Huang, N.-P.; Michel, R.; Voros, J.; Textor, M.; Hofer, R.; Rossi, A.; Elbert, D. L.; Hubbell, J. A.; Spencer, N. D., Poly(L-lysine)-g-poly(ethylene glycol) Layers on Metal Oxide Surfaces: Surface-Analytical Characterization and Resistance to Serum and Fibrinogen Adsorption. *Langmuir* **2001,** *17*, 489-498.

Jalonick, M. C., Salmonella confirmed in peanut butter plant. *Associated Press* October 5, 2012.

Jeyachandran, Y. L.; Mielczarski, E.; Rai, B.; Mielczarski, J. A., Quantitative and Qualitative Evaluation of Adsorption/Desorption of Bovine Serum Albumin on Hydrophilic and Hydrophobic Surfaces. *Langmuir* **2009,** *25* (19), 11614-11620.

Jin, T.; Zhang, H., Biodegradable Polylactic Acid Polymer with Nisin for Use in Antimicrobial Food Packaging. *Food Microbiology and Safety* **2008,** *73* (9).

Kiss, E.; Dravetzky, K.; Hill, K.; Kutnyanszky, E.; A., V., Protein interaction with a Pluronic-modified poly9lactic acid) Langmuir monolayer. *Journal of colloid and Interface Science* **2008**.

Mauriello, G.; De Luca, E.; La Storia, A.; Vallani, F.; Ecrolini, D., Antimicrobial activity of a nisin-activated plastic film for food packaging. *Letters in Applied Microbiology* **2005,** *41*, 464-469.

McPherson, T. B.; Shim, H. S.; Park, K., Grafting of PEO to glass, nitinol, and pyrolytic carbon surfaces by γ irradiation. *Journal of Biomedical Materials Research* **1997,** *38*.

Norde, W.; Gage, D., Interaction of Bovine Serum Albumin and Human Blood Plasma with PEO-Tethered Surfaces: Influence of PEO Chain Length, Grafting Density, and Temperature. *Langmuir* **2004,** *20*, 4162-4167.

Norde, W.; Giacomelli, C. E., BSA structural changes during homomolecular exchange between the adsorbed and the dissolved states. *Journal of Biotechnology* **2000,** *79*, 259-268.

Popat, K. C.; Johnson, R. W.; Desai, T. A., Characterization of vapor deposited thin silane film on silicon substrates for biomedical microdevices. *Surface and Coatings Technology* **2002,** *154*, 253-261.

Popat, K. C.; Sadhana, S.; Johnson, R. W.; Desai, T. A., AFM analysis of organic silane thing films for bioMEMS applications. *Surface and Interface Analysis* **2003,** *35*, 205-215.

Prombutara, P.; Kulwatthanasal, Y.; Spaka, N.; Sramala, I.; Chareonpornwattana, S., Production of nisin-loaded solid lipid nanoparticles for sustained antimicrobial activity. *Food Control* **2002,** *24*, 184-190.

Quintavalla, S.; Vicini, L., Antimicrobial food packaging in meat industry. *Meat Science* **2002,** *62*, 373-380.

Ruhr, E.; Sahl, H.-G., Mode of action of the peptide antibiotic nisin and influence of the membrane potential of whole cells and on cytoplasmic and artificial membrane vesicles. *Antimicrobial Agents and Chemotherapy* **1985,** *27*, 841-845.

Ryder, M. P.; Schilke, K. F.; Auxier, J. A.; McGuire, J.; Neff, J. A., Nisin adsorption to polyethylene oxide layers and its resistance to elution in the presence of fibrinogen. *Journal of Colloid and Interface Science* **2010,** *350* (1), 194-199.

Salmaso, S.; Elvassore, N.; Bertucco, A.; Lante, A.; Caliceti, P., Nisin-loaded poly-l-lactide nano-particles produced by CO2 anti-solven$_t$ precipitation for sustained antimicrobial activity. *International Journal of Pharmaceutics* **2004,** *287* (1-2), 163-173.

Salmio, H.; Bruhwiler, D., Distribution of amino groups on a mesoporous silica surface after submonolayer deposition of aminopropylsilanes from an anhydrous liquid phase. *Journal of Physical Chemistry* **2007,** *C111*.

Schilke, K. F.; McGuire, J., Detection of nisin and fibrinogen adsorption on poly (ethylene oxide) coated polyurethane surfaces by time-of-flight secondary ion mass spectrometry (TOF-SIMS). *Journal of colloid and interface science* **2011**.

Sofia, S. J.; Premnath, V.; W., M. E., Poly(ethylene oxide) Grafted to Silicon Surfaces: Grafting Density and Protein Adsorption. *Macromolecules* **1998,** *31*, 5059-5070.

Székács, A.; Adányi, N.; Székács, I.; Majer-Baranyi, K.; Szendrö, I., Optical waveguide light-mode spectroscopy immunosensors for environmental monitoring. *Applied Optics* **2009,** *48* (4), B151-B159.

Tai, Y. C.; Joshi, P.; McGuire, J.; Neff, J. A., Nisin adsorption to hydrophobic surfaces coated with the PEO-PPO-PEO triblock surfactant Pluronic (R) F108. *Journal of Colloid and Interface Science* **2008,** *322* (1), 112-118.

Tai, Y.-C.; McGuire, J.; Neff, J., Nisin antimicrobial activity and structural characteristics at hydrophobic surfaces coated wit the PEO-PPO-PEO triblock surfactant Pluronic® F108. *Journal of Colloid and Interface Science* **2008,** *322* (1), 104-111.

Tie, Y.; Ngankam, P.; Van Tassel, P. R., Probing Macromolecular Adsorbed Layer Structure and History Dependence via the Interfacial Cavity Function. *Langmuir* **2004,** *20*, 10599-10693.

Tseng, Y.-C.; McPherson, T.; Yuan, C. S.; Park, K., Grafting of ethylene glycol-butadiene block copolymers onto dimethyl-dichlorosilane-coated glass by γ-irradiation. *Biochemistry* **1995,** *16*.

Tsukagoshi, T.; Kondo, Y.; Yoshino, N., Protein adsorption and stability of poly(ethylene oxide)-modified surfaces having hydrophobic layer between substrate and polymer. *Colloids and Surfaces B: Biointerfaces* **2007,** *54*, 82-87.

Unsworth, L. D.; Sheardown, H.; Brash, J. L., Polyethylene oxide surfaces of variable chain density by chemisorption of PEO-thiol on gold: Adsorption of proteins from plasma studied by radiolabelling and immunoblotting. *Biomaterial* **2005,** *26* (30), 5927-5933.

Unsworth, L. D.; Sheardown, H.; Brash, J. L., Protein-Resistant Poly(ethylene oxide)-Grafted surfaces: Chain Density-Dependent Multiple Mechanisms of Action. *Langmuir* **2008,** *24*, 1924-1929.

Wertz, C. F.; Santore, M. M., Fibrinogen Adsorption on Hydrophilic and Hydrophobic Surfaces: Geometrical and Energetic Aspects of Interfacial Relaxations. *Langmuir* **2002,** *18* (706-715).

Wiedemann, I.; Breukink, E.; van Kraaij, C.; Kuipersi, O. P.; Bierbaum, G.; de Krujiff, B.; Sahl, H.-G., Specific Binding of Nisin to the Peptidoglycan Precursor Lipid II Combines Pore Formation and Inhibition of Cell Wall Biosynthesis for Potent Antimicrobial Activity. *The Journal of biological Chemistry* **2001,** *276* (1), 1776-1779.

Zou, Y.; Lee, H.-Y.; Seo, Y.-C.; Ahn, J., Enhanced antimicrobial activity of nisin-loaded liposomal nanoparticles against foodborne pathogens. *Journal of Food Science* **2012,** *77* (3).

APPENDICES

APPENDIX A

SURFACE MODIFICATION AND LAYER CREATION METHODS

A.1 Silanization of Silica

A lab scale vapor deposition device, OSCAR, was used for silane vapor deposition. The process has been optimized during extensive previous research projects. Liquid-based modification was also conducted for silica microspheres using TCVS in chloroform; because the process was not frequently executed and the existing procedure was successful, it was not optimized. The vapor silanization for all experiments was performed by the following process.

Flat silica surfaces, either wafers (1 cm^2, WaferNet, San Jose, CA) or SiO_2 coated OWLS sensors, were thoroughly cleaned to remove surface impurities. Wafers were RCA (Radio Corporation of America) cleaned: a base wash (5:1:1 H_2O:NaOH:H_2O_2) followed by an acid wash (5:1:1 H_2O:HCl:H_2O_2) for 10 min each in an 80 °C bath with H_2O rinsing between washes. OWLS sensors were immersed in chromosulfuric acid for 15 min and rinsed with H_2O. All surfaces were then rinsed with ethanol to molecularly dehydrate the surface and blown dry with nitrogen to remove bulk water. Surfaces were uniformly spaced in the reaction chamber of OSCAR. Nitrogen was passed through OSCAR for at least 30 min to equilibrate the system and remove any last water from the surfaces.

Tricholorvinylsilane (TCVS) is a silane that produces siloxane reactive groups on a surface. It is highly reactive with water and will polymerize in the presence of water. For this reason, the surfaces were meticulously dried to achieve as uniform a coating as possible. After equilibrating the system, TCVS (Sigma, 104876) was injected into the reagent chamber using a plastic syringe and plastic tip punctured through a septum. Once injected, the syringe was left in the septum for the duration of the process. Nitrogen was then circulated through for at least 2 h through the reagent chamber and to the reaction chamber to carry volatilized TCVS over the surfaces. After silanization, surfaces were cured at 120 °C to stabilize the coating.

A.2 Polyethyleneoxide immobilization and nisin entrapment

The reactive siloxanes render the surface hydrophobic. Polyethyleneoxide forms self-assembled monolayers (SAMs) on hydrophobic surfaces. Therefore, PEO self assembles on the modified silica. The PEO could then be covalently stabilized by gamma-irradiation (Figure A.1). The surfaces were immersed in a PEO solution of 5% F108 in PBS (10 mM with 150 mM NaCl) or 5% F68 in PBS with additional salt (10 mM with 400 mM NaCl). Problems creating F68 layers in previous work were mediated by the addition of salt which causes the PEO to crash to the surface. While in the PEO solutions, surfaces were gamma irradiated (0.3 Mrad). Post irradiation surfaces were left in the dark to minimize any potential UV degradation.

Bioactive function can be imparted to the non-fouling PEO coatings by nisin integration - the method of entrapment is discussed at length in Chapter 2. The nisin solution preparation required particular attention to detail. The nisin was thawed to room temperature before adding to monobasic buffer (10 mM with 150 mM NaCl). The solution was then rotated at 37 °C until dissolved (generally multiple hours). Once dissolved, dibasic was added for a final ratio of 19:81 monobasic to dibasic (final pH of ~7.4) and 0.5 mg/mL nisin concentration. Excess PEO was rinsed from immobilized PEO surfaces with water before immersion in nisin solution for at least 4 h. Excess nisin was rinsed with H_2O before use.

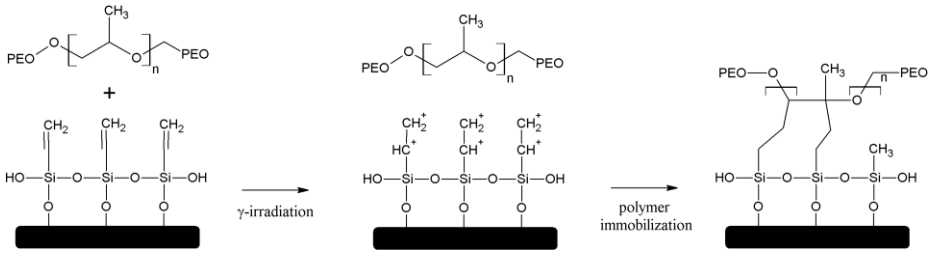

Figure A.1: Immobilization of PEO onto free silanols on TCVS silanized silica.

APPENDIX B

QUANTIFICATION OF RELATIVE ACTIVITIES OF FREE AND ENTRAPPED NISIN AGAINST *P. PENTOSACEUS* AND *S. EPIDERMIDIS*

B.1 Bacterial preparation

B.1.1 *Pediococcus pentosaceus*

A stock culture *Pediococcus pentosaceus* was prepared according to manufacturer's instructions prior to the start of work described herein. A working culture was prepared from the stock culture for each activity test. All subcultures were prepared from the working culture for the duration of activity test (B.1.3 *Culture Preparation*).

A standard curve of absorbance versus concentration of *P. pentosaceus* was prepared by measuring the absorbance and dry weight of overnight culture dilutions (Figure B.1). The best linear range falls between 0.5 and 1.1 (OD600) and correlates to previous lab work presented in Tai, *et al*.

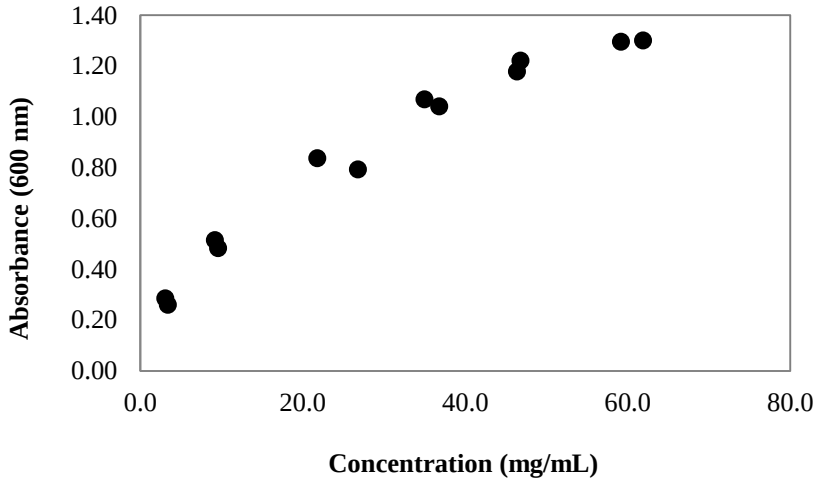

Figure B.1: Absorbance of *P. pentosaceus* overnight culture versus culture concentration.

B.1.2 *Staphylococcus epidermidis*

A stock culture of *Staphylococcus epidermidis* (ATCC 12228) was prepared according to manufacturer's instructions. A working culture was prepared from the stock culture for each activity test. All subcultures were prepared from the working culture for the duration of the test (B.1.3 *Culture Preparation*).

A standard curve of absorbance versus concentration of *S. epidermidis* was prepared measuring the absorbance and dry weight of overnight culture dilutions (Figure B.2). A linear correlation was found within the range tested (R^2= 0.984).

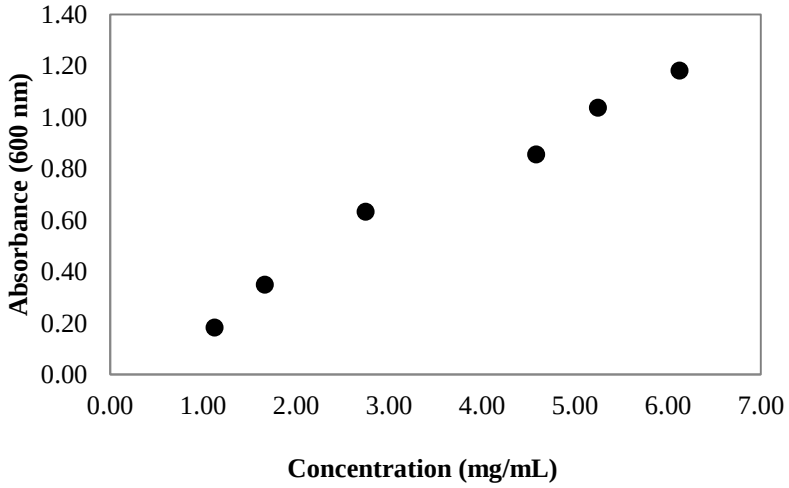

Figure B.2: Absorbance of *S. epidermidis* overnight culture versus culture concentration.

B.1.3 *Culture preparation*

Media for all experimentation was sterilely prepared for each experiment. Media powder was fully dissolved in HPLC or nanopure water, depending on availability. MRS boullion (52.2 g/L) was used for *P. pentosaceus* cultures and NB powder (8 g/L) was used for

S. epidermidis cultures. Media was covered and autoclaved for 30 min. After sterilization, media was never handled outside of the laminar flow hood.

Working cultures were prepared for each experiment, which lasted approximately one month or less. A vial of stock culture bacteria was thawed at ambient temperature until fully liquid. A sterile inoculating loop was used to transfer a loop of stock bacteria to a culture vial containing 6 mL of sterile media and then cultured overnight at 37 °C on a gently rotating orbital shaker. The overnight culture was then spread-plated on a sterile agar Petri plate (1% w/v agar) with a sterile inoculating loop so as to isolate individual colonies. The spread plate was then incubated at 37 °C overnight. The final working culture was sealed and kept at 4 °C until needed and was resealed and returned to 4 °C after use.

All overnight cultures were prepared in the following method. Sterile media was added to culture vial (6 mL/vial). For each culture vial, a sterile inoculating loop was used to remove a single colony from the bacteria working culture and added to the culture tube. Culture tubes were loosely capped to prevent particulate contamination but also to allow for gas exchange. Culture tubes were then placed in a temperature controlled orbital shaker set at 37 °C and gently shaken overnight (at least 12 h) until culture absorbance fell within linear range. All work was conducted in a laminar flow hood.

B.2 Colony Forming Units (CFU) determination for bacterial strains

The colony forming units for *S. epidermidis* and *P. pentosaceus* were determined using a plated dilution technique. CFU correlation to absorbance allows for controlled sample inoculation and quantification.

Agar (Difco) was dissolved in MRS broth (52.2 mg/mL) and NB broth (8 g/L) to 1% w/v and sterilized by autoclave. Plates were poured and allowed to set. Serial dilutions (10^{0}-10^{-8}) of overnight cultures were prepared with respective broths, MRS broth for *P. pentosaceus* and NB broth for *S. epidermidis*. 20 µL of each dilution were dispensed onto a plate from 2-3 cm above the plate. Plates were left to dry upright in laminar flow hood before placing in 37 °C incubator overnight.

Confluence was observed on for dilution factors 10^{0}-10^{-4} for both *P. pentosaceus* and *S. epidermidis*. Individual colonies were apparent starting at the 10^{-5} dilution. The CFU's were calculated to be $3.46 \cdot 10^{5}$ CFU/mL for *P. pentosaceus* and $2.07 \cdot 10^{5}$ CFU/mL for *S. epidermidis*.

B.3 Minimum inhibitory concentration for bacterial strains

The minimum inhibitory concentration (MIC) of nisin against each bacterial strain under different buffer conditions was determined to choose the optimal conditions for activity assays.

Nisin was dissolved in either PBS at pH 7 or phosphate citrate buffer at pH 4 to a final concentration of 0.5 mg/mL. The nisin solutions were then serially diluted from 10^{0}-10^{-8} in PBS at pH 7 or phosphate citrate bugger at pH 4. 50 µL of the dilutions were combined with 50 µL of *P. pentosaceus* or *S. epidermidis* in a 96-well plate. Well plates were placed in a 37 °C incubator overnight after which the absorbance (280 nm) of each was measured.

The results for nisin against *P. pentosaceus* clearly showed a MIC, but nisin against *S. epidermidis* did not yield clear results. The range of concentrations tested may have been below the MIC or the test may have not been sensitive enough to detect the MIC for nisin against *S. epidermidis*. Continual troubles working with *S. epidermidis* led to preferential use of *P. pentosaceus* as the indicator strain for activity tests. The calculated MIC's for the different buffer conditions against *P. pentosaceus* are presented and discussed in Chapter 3.

B.4 Attempts at INT stain

It was desired to quantify bacterial viability using an alternative method to plated diffusion kill zones, namely by viability staining. In past work, nisin activity against *L. monolisteria* was quantified using iodonitrotetrazolium (INT) staining. The INT available was originally used in Bower *et al*.

INT (Sigma, I10406) was added to HPLC water heated to 50 °C and dissolved in the dark (multiple hours) to 2 mg/mL and stored at 4 °C until needed. Overnight cultures of both *P. pentosaceus* and *S. epidermidis* were prepared. The overnight cultures were divided and one half autoclaved (inactivated). Microscope slides were cleaned with ethanol and allowed to dry in a sterile laminar flow hood. INT solution and overnight culture, active and inactivated, were mixed 1:1 on the microscope slide. Coverslips were placed on top of the mixed solution and allowed to react for 15 min. Samples were visualized using oil immersion on a light microscope.

INT staining did not yield positive results: both active and inactivated samples stained identically. The failure of this initial attempt was attributed to degradation of the available INT. INT solutions are quoted to have a shelf life of two years and the available solution was over 12 years old. Readily available trypan blue stain was substituted as an alternative staining technique.

Trypan blue solution was added 1:1 to overnight cultures, active and inactivated, covered with a coverslip, and allowed to react for 15 min. The samples were again visualized using oil immersion on a light microscope.

The active cultures of *P. pentosaceus* and *S. epidermidis* did not stain (the cells were opalescent, clear). The autoclaved *P. pentosaceus* culture stained blue, indicating the bacteria membrane was no longer functioning and the bacteria were killed. However, the autoclaved *S.*

epidermidis culture did not stain blue, indicating the bacteria were not inactivated, or that the trypan blue stain did not function. In order to eliminate the possibility that autoclaving did not kill the *S. epidermidis*, the overnight cultures were exposed to 10% bleach solution for at least 2 h before repeating the trypan blue staining process. Again, the live cultures remained opalescent, the inactivated *P. pentosaceus* sample stained blue, and the inactivated *S. epidermidis* sample did not stain blue.

It is possible that the trypan blue solution was also no longer usable for it was multiple years older than the suggested shelf-life of trypan blue, approximately six months after initial use (T8154). It is also possible that trypan blue was not an appropriate stain for indicating viability. The commercially available LIVE/DEAD® BacLight™ bacterial viability kit would be an apt technique for the desired purpose. Further investigation and process optimization was clearly necessary, but due to time constraints the staining process was abandoned.

B.5 Nisin activity against *P. pentosaceus* and *S. epidermidis*

The following section presents the chronology of activity experiments that led up to the successful activity assay presented in Chapter 3. The activity of nisin was quantified using plated diffusion kill zone radii on a bacterial lawn. Nisin in solution is henceforth denoted as "free nisin" and nisin integrated into a brush layer is termed "entrapped nisin." Nisin activity was expected to decrease over time when exposed to other proteins.

The process began with free nisin activity against *P. pentosaceus* and progressed to a first attempt of the entrapped nisin assay. Extensive troubleshooting and parameter optimization then followed in the forms of multiple free and entrapped nisin activity assays. The chronology is meant to provide insight on the inner workings and limitations of the model system.

B.5.1 Unchallenged free nisin activity against *P. pentosaceus*

Initially, the diffusion halo assay was performed using free nisin dilutions in PBS, pH ~7, at 37 °C for a week in order to test the mechanics of the assay and determine if nisin activity loss could be measured at extreme dilutions. This experiment was conducted prior to determination of nisin MIC against *P. pentosaceus* at different buffer pH values.

A 0.5 mg/mL nisin solution was prepared in PBS as previously described (Appendix A). The nisin was held at 37 °C for the duration of the experiment. Every 4 days nisin was removed from the incubator and a portion diluted by a factor of 10^9. 10 µL of 0.5 mg/mL nisin and 10^{-9} nisin dilution were dropped onto circle of filter paper 6 mm in diameter. The volume added was fully absorbed by the filter paper.

Nisin soaked filter papers were then plated against *P. pentosaceus* inoculated agar plates (1 mg/mL *P. pentosaceus* in media). Sterile agar plates were prepared and overnight culture started the day before plating. The overnight culture was spread plated (commonly

termed the “hockey stick method”) and the nisin soaked filter papers added to the center of the plate. Covered plates were placed in the 37 °C incubator overnight and kill zone radii measured. The kill zone was defined as the distance to bacterial growth extending beyond the perimeter of the filter paper (or wafer in later tests). Proper negative controls were also plated for each sampling day: plates containing no nisin but still inoculated, or no nisin and not inoculated.

No contamination, indicated by growth on negative controls, was observed through the entire experiment. Kill zones of ~1.7 cm were initially observed in both 0.5 mg/mL and 10^{-9} diluted nisin solutions. The kill zones for nisin at 0.5 mg/mL were still present after 12 days of incubation at 37 °C. The change in kill zone over time was not substantial and measurement of any change would be beyond the accuracy possible for the test; kill zones were only quantified to the nearest millimeter. Conversely, the diluted nisin activity continually decreased throughout the 12 days until no activity was observed on the 12^{th} day.

It was concluded that nisin does not quickly lose activity at 37 °C even at low concentrations. Additionally, activity loss was more easily tracked in the more dilute nisin solution (Figure B.3). Therefore, the assay was validated and expected to work for nisin entrapped in F108 layers because low nisin concentrations were expected for the given, small surface area.

a) b)

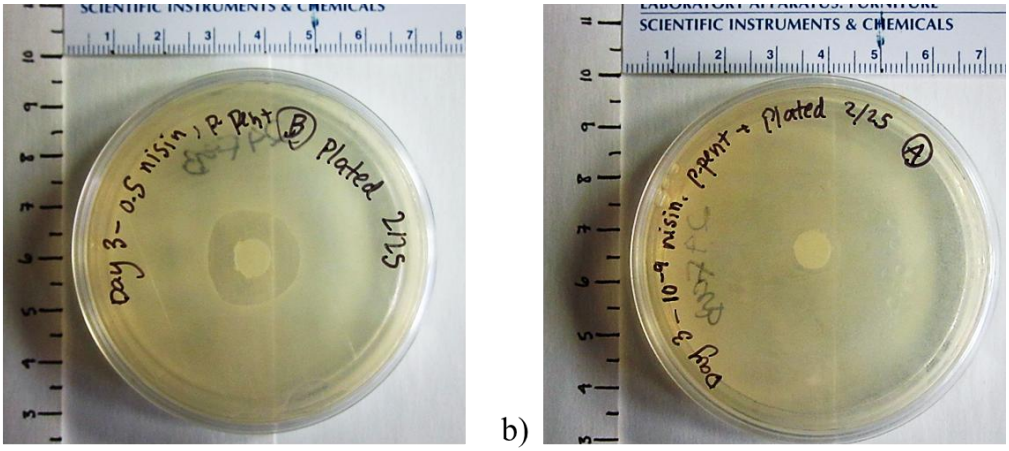

Figure B.3: a) 0.5 mg/mL nisin solution and b) 10^{9} nisin dilution were added to filter paper and plated against *P. pentosaceus* after 4 days incubation at 37 °C. Both showed activity, but the loss of activity over time was more noticeable in the 10^{-9} nisin dilution. The results validate the assay for the model surfaces.

B.5.2 Plasma challenged, entrapped nisin activity against *S. epidermidis*

S. epidermidis is a clinically relevant organism and nisin activity retention against such an organism would make these coatings attractive for medical applications. It was recognized that nisin is not as active at higher pH but given the measurable activity of very low nisin concentrations, it was expected that some activity would be observed. An attempt was made to measure activity retention in entrapped nisin versus surface bound nisin challenged with plasma and tested against *S. epidermidis*.

Model surfaces were silanized, coated with F108 (5% w/v in PBS), and exposed to nisin (0.5 mg/mL in PBS) as described previously (Appendix A). The F108 immobilized surfaces and the nisin solution were previously prepared for a separate experiment. Fresh solutions and surfaces were not created because this attempt was viewed as a "trial run" of the experiment. The wafers were placed in well plate wells, covered with equine plasma (Hemostat) diluted to 25% with water, and incubated at 37 °C. Every three days, wafers were

removed from the plasma, thoroughly rinsed with water, and plated on *S. epidermidis* inoculated agar. The bacterial cultures and plates were prepared in the same manner as the free nisin assay.

No kill was observed the first day. It was thought that perhaps the nisin solution used to coat the wafers was compromised and a fresh solution would yield better results. As a quick test to determine if fresh nisin had any effect on *S. epidermidis*, surface adsorbed nisin from a fresh nisin solution was exposed to plasma and plated against *S. epidermidis*. Fresh 0.5 mg/mL nisin in PBS solution was prepared and adsorbed to RCA cleansed silica wafers. The nisin-coated wafers were placed in well plate wells and 25% plasma added to cover. These wafers were plated against *S. epidermidis* in the same manner described above.

The surface adsorbed nisin wafers exhibited activity against *S. epidermidis* before being challenged with 25% equine plasma; faint 2-3 mm kill zones were observed. However, insignificant activity was observed once the surfaces were challenged with the diluted plasma. It was abundantly clear that parameter optimization would be absolutely necessary to succeed. The sensitivity of *S. epidermidis* to nisin and the inoculum concentration were investigated more in depth.

B.5.3 Unchallenged free nisin activity against *S. epidermidis*

The free nisin assay was performed against *S. epidermidis* to determine if nisin could exhibit activity against the strain, if it was only substantially effective against *P. pentosaceus*, and if active what concentration of nisin was needed to exhibit measurable activity. The relative sensitivities of *P. pentosaceus* and *S. epidermidis* to nisin would indicate the proper indicator strain needed for successful measure of activity retention. If the nisin showed minimal effect against *S. epidermidis* using the given assay, the system would be treated as a model and the purpose of the work would focus more on proof of concept.

An experimental design similar to the assay of free nisin activity against *P. pentosaceus* was applied. Fresh 0.5 mg/mL nisin solution was diluted 1x, 2x, 10x, and 100x. Circles of filter paper, 6 mm in diameter, were soaked in the dilutions, plated against *S. epidermidis* inoculated (~1mg/mL) plates, and incubated at 37 °C overnight. Activity was observed for 1-10x dilutions, but not for 100x.

For the 1 mg/mL inoculation concentration, nisin at least 0.05 mg/mL or greater would be needed for measurable activity: much more than the concentration required for measurable activity against *P . pentosaceus*. This result is expected since the MIC of nisin is lower for *P. pentosaceus* than for *S. epidermidis*. In order to increase visible activity against *S. epidermidis*, it was thought that the inoculation concentration could be decreased to increase observed activity (increase kill zone halos).

Filter paper circles soaked with 0.5 mg/mL nisin were plated against agar plates with serial dilutions of 1 mg/mL *S. epidermidis* inoculation concentrations from 10^{0}-10^{-5} and incubated at 37 °C in the same manner as previous tests. Increased kill zones were observed as inoculation concentration decreased. However, a limit was reached for maximum kill zone and at the lowest dilutions individual colonies formed in the agar instead of a confluent bacterial lawn. It was determined that for optimal measurable activity future tests with *S. epidermidis* would have a 0.02 mg/mL inoculation concentration.

B.5.4 Free nisin activity against *S. epidermidis* and *P. pentosaceus*

A final comparison of free nisin activity using 1 mg/mL inoculation concentrations of both bacterial strains was conducted to finalize relative nisin activities and validate abandoning *S. epidermidis* in favor of *P. pentosaceus*. Again, filter paper circles soaked with 0.5 mg/mL nisin solution in PBS were plated against both strains (1 mg/mL inoculation concentration) and incubated overnight at 37 °C. Indeed, substantially greater activity was

observed for *P. pentosaceus* over *S. epidermidis*: 2-2.5 cm halo against *P. pentosaceus* compared to 0.25-0.5 cm halo against *S. epidermidis* (Figure B.4).

a) 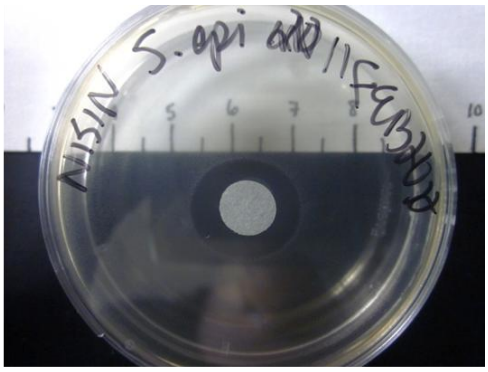 b) 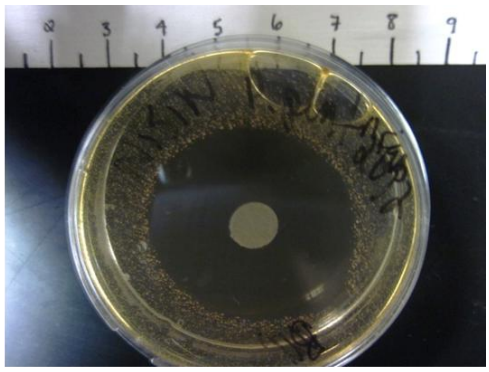

Figure B.4: Filter papers containing the same amount of nisin were plated against a) *S. epidermidis* and b) *P. pentosaceus*. Nisin was more effective against *P. pentosaceus*.

The experimentally determined CFUs of overnight cultures of the two bacterial strains were in the same order of magnitude and so it may be concluded that equal inoculation concentrations (mg/mL) contain approximately comparable CFUs of bacteria between the two strains. Therefore, the distinctly lower kill zones against *S. epidermidis* indicate that nisin is less effective and modeling the system would best be done with *P. pentosaceus*.

B.5.5 Plasma challenged, entrapped nisin activity against *P. pentosaceus* and *S. epidermidis*

With the information gleaned from the parameter optimizations, activity of nisin entrapped in immobilized F108 layers when challenged with 25% equine plasma was to be quantified using the diffusion halo assay against *P. pentosaceus* and *S. epidermidis*. Silica wafers were modified with gamma-irradiated F108 and coated with nisin in the same manner as described in Appendix A. Wafers were placed in wells of well plates, covered with 25% equine plasma, and incubated at 37 °C. At set time intervals wafers were plated on agar plates

inoculated with 1 mg/mL *P. pentosaceus* and 0.02 mg/mL *S. epidermidis* and incubated at 37 °C overnight.

After one day of incubation, both surfaces with nisin (with and without F108) exhibited activity against ***both*** *P. pentosaceus* and *S. epidermidis*. However, after three days no kill was observed for any of the surfaces. Again, it was abundantly clear that some part of the assay was askew. The nisin may have been compromised for it was not a newly prepared solution. The surfaces were also not newly made. Finally, due to the small surface area and therefore small quantity of nisin on the wafer surface, the plasma may have inactivated nisin too quickly. If there was increased surface area, such as with microspheres, more nisin would be present, the activity "signal" would be amplified, and then perhaps a measurable amount of activity against *S. epidermidis* after challenging with diluted plasma would be possible. With the microsphere geometry, the activity could be quantified using spectrophotometry of cultures. However, time did not allow for the development and optimization of another biological assay.

B.5.6 Conclusions

At this point the entire endeavor was reevaluated. The model system had many limitations: limited surface area and nisin loading, bacterial sensitivity differences, difficulty preparing nisin solutions, and time constraints. Measures were taken to mediate these limitations through parameter optimization. However, the system was too complex and needed to be reduced to a simpler model. The concept of nisin activity retention when entrapped in PEO brush layers had to be proved before advancing to more a complex system. With knowledge gained from these preliminary tests the purpose of the activity tests was redefined. The purpose was no longer to prove retained activity of entrapped nisin against the clinically

relevant *S. epidermidis*, but to prove that entrapment in F108 brush layers retains nisin activity longer than surface bound nisin.

APPENDIX C

NISIN ADSORPTION TO POLYETHYLENE OXIDE LAYERS AND ITS RESISTANCE TO ELUTION IN THE PRESENCE OF FIBRINOGEN

Matthew P. Ryder[a], Karl F. Schilke[a], Julie A. Auxier[a], Joseph McGuire[a,*] and Jennifer A. Neff[b]

[a] School of Chemical, Biological and Environmental Engineering, Oregon State University, Corvallis, OR 97331

[b] Allvivo Vascular, Inc., Lake Forest, CA 92630

*Corresponding author: joseph.mcguire@oregonstate.edu;
541-737-4600 (fax);
541-737-6306 (tel)

J. Colloid Interface Sci. 350:194-199, 2010

Abstract

The adsorption and elution of the antimicrobial peptide nisin at silanized silica surfaces coated to present pendant polyethylene oxide chains was detected *in situ* by zeta potential measurements. Silica microspheres were treated with trichlorovinylsilane to introduce hydrophobic vinyl groups, followed by self assembly of the polyethylene oxide-polypropylene oxide-polyethylene oxide (PEO-PPO-PEO) triblock surfactant Pluronic® F108, or an F108 derivative with nitrilotriacetic acid endgroups. Triblock-coated microspheres were γ-irradiated to covalently stabilize the PPO-surface association. PEO layer stability was evaluated by triblock resistance to elution by SDS, and layer uniformity was evaluated by fibrinogen repulsion. Introduction of nisin to uncoated or triblock-coated microspheres produced a significant positive change in surface charge (zeta potential) as a result of adsorption of the cationic peptide. In sequential adsorption experiments, the introduction of fibrinogen to nisin-loaded triblock layers caused a decrease in zeta potential that was consistent with partial elution of nisin and/or preferential location of fibrinogen at the interface. This change was substantially more pronounced for uncoated than triblock-coated silica, indicating that the PEO layer offers enhanced resistance to nisin elution.

Keywords: nisin adsorption; zeta potential; Pluronic® F108; PEO-PPO-PEO triblock surfactant; EGAP-NTA

C.1 Introduction

Nisin is a small (3.4 kDa) amphiphilic peptide with five lanthionine rings. It is cationic at neutral pH, due to an isoelectric point above 8.5. Nisin is an effective inhibitor of Gram-positive bacteria, including the two most frequently encountered biomaterial-associated pathogens *Staphylococcus aureus* and *Staphylococcus epidermidis* [1-3], and holds potential for use as an anti-infective agent in medical device coatings [4, 5].

Tai *et al*. [6] reported results of an ellipsometric analysis of nisin adsorption and elution at surfaces coated with the PEO-PPO-PEO surfactant Pluronic® F108. Those results suggested that nisin adsorption occurred via penetration of and entrapment within the PEO layer, as opposed to adsorption onto the mobile PEO chains. It is generally understood that PEO resists protein interactions, and the protein repellent properties of the F108 layer, if retained after nisin adsorption or integration, would inhibit displacement of the antimicrobial peptide by blood proteins. In this way, nisin loading could impart an active protective function, and increase the effectiveness of such a coating. In this regard Tai *et al*. [7] evaluated the antimicrobial activity of nisin-loaded, F108-coated polystyrene microspheres and polyurethane catheter segments after incubation with blood proteins for up to one week. F108-coated surfaces were observed to retain more antimicrobial activity than uncoated surfaces, suggesting that the pendant PEO chains inhibited displacement or elution of nisin by contact with blood proteins.

The F108 triblocks used by Tai *et al*. were bound to the base substrates only by hydrophobic association of the polymer and PPO centerblock. It is thus possible that adsorbing nisin dislocated the adsorbed Pluronic at the surface, rather than being integrated into the brush layer itself. Important conclusions relating to nisin entrapment among PEO chains, as well as the enhanced resistance to elution of nisin bound in this way, have thus

remained somewhat tentative. In this paper we describe the individual and sequential adsorption of nisin and fibrinogen at silanized silica surfaces coated with covalently-bound PEO-PPO-PEO triblocks. Zeta potential was recorded after protein adsorption to microsphere suspensions coated with F108, or with F108 that had been end-activated with nitrilotriacetic acid groups (EGAP-NTA).

While an abundant literature describes the protein repelling mechanisms of material surfaces presenting pendant PEO, there are very few reports describing the adsorption of small proteins to PEO layers. It has been argued that once a sufficiently high chain density is achieved, the rejection capacity of the pendant polymer phase is determined by protein size, relative to the average distance between polymer chains [8, 9]. Archambault and Brash [10] suggested that grafting densities consistent with the brush configuration would be required before protein discrimination based on size would become evident. Halperin [11] formulated a model for protein adsorption in a PEO brush based on kinetic and thermodynamic considerations, and predicted two possible modes of protein adsorption: primary adsorption (at the surface itself) and secondary adsorption (at the periphery of the grafted PEO chains). Multilayer formation or integration of protein within the PEO chains is not predicted by this simplified model. However, based on surface force experiments involving compression of PEO brushes by protein-coated surfaces, Sheth and Leckband [12] suggested that polymer chains in a PEO brush may exhibit coexistence between an inner, dense, hydrophobic phase and a dilute hydrophilic phase at the outer edge of the brush. Such coexistence would give rise to an inner region “attractive” for protein adsorption. Nisin adsorption within PEO layers may thus be attributable to its high amphiphilicity, in addition to its small size.

Fang *et al*. [13] formulated a model for protein interaction with PEO brushes based on a generalized diffusion approach. Their model showed that adsorption and desorption kinetics

depend on protein size and brush layer thickness. In particular, when the pendant chain layer thickness is greater than the size of the protein, adsorption and desorption kinetics both decrease with increasing chain length. In fact, their model indicated that the adsorption time is so large that, for any practical purpose, protein adsorption is negligible. A particularly interesting outcome of their approach was that proteins may become "trapped" between the surface and the barrier presented by the pendant chains. Increasing the chain length increases the steric barrier to elution, and the rate of protein desorption is thus decreased. Based on that result, they suggested that such a trapping mechanism could be used in the design of strategies for the controlled release of proteins from surfaces.

Some studies have shown that protein adsorption is insensitive to PEO end group chemistry while others have reported significant effects. Mathematical models of PEO in the brush configuration indicate that it is highly unlikely that end group chemistry would affect interaction with proteins. For example, Halperin [11] showed that chain ends are statistically distributed throughout the brush, with a maximum occurring at a distance about 70% of the chain length from the surface. Unsworth *et al*. [14] showed experimentally that protein repulsion at PEO brushes was uniquely determined by chain density, independent of chain length and end group chemistry. However, beyond a critical chain density, it was observed that brushes with –OH end groups were observed to remain nonfouling, while brushes with –OCH_3 end groups promoted protein adsorption. The authors suggested that the high densities of terminal methoxy groups may have resulted in increased inter-chain association and/or adsorption-induced protein denaturation. The formation of terminal –OCH_3 "islands" and defects in the brush layer are also predicted theoretically in a random-sequential-adsorption model advanced by Katira *et al*. [15].

C.2 Materials and Methods

C.2.1 Proteins and surfactants

A commercial purified nisin preparation was obtained from Prime Pharma (Gordons Bay, South Africa), and was dissolved as needed in filtered (0.2 μm), 10 mM monobasic sodium phosphate solution with 150 mM NaCl. To this was added filtered, 10 mM dibasic sodium phosphate with 150 mM NaCl to bring the pH to 7.4. Fibrinogen (MW 340 kDa, Sigma-Aldrich, St. Louis, MO) was dissolved in filtered, 10 mM phosphate-buffered saline (150 mM NaCl, pH 7.4, PBS), incubated at 37 °C for 4 h with gentle mixing, and then passed through a 0.45 □m syringe filter to remove aggregates. All protein solutions were prepared immediately prior to use. BASF Pluronic® triblock surfactant F108 (PEO_{141}–PPO_{44}– PEO_{141}), and an end-group activated form of Pluronic® F108, with the terminal hydroxyl groups of the PEO chains converted to nitrilotriacetic acid groups (EGAP-NTA), were obtained from Allvivo Vascular, Inc. Polyclonal anti-human fibrinogen antibodies modified with horseradish peroxidase (HRP) were purchased from U.S. Biological (Swampscott, MA). All other reagents and solvents were purchased from commercial sources, and were of the highest practical purity. All solutions and buffers were made with HPLC-grade H_2O to minimize contamination.

C.2.2 Silica surface modification

Monodisperse, 1 μm silica microspheres (Fiber Optic Center, New Bedford, MA) were used as the base substrate for all zeta potential measurements. The microspheres were washed with H_2O:30% NH_4OH:30% H_2O_2 (5:1:1 v/v) at 80 °C for 10 min, followed by H_2O:37% HCl:30% H_2O_2 (5:1:1 v/v) at 80 °C for 10 min to remove organic contaminants [6]. The washed (bare) microspheres were then rinsed with H_2O three times, dried at 110 °C, and stored desiccated.

The washed microspheres were modified to render the silica surfaces sufficiently hydrophobic for triblock coating with two different, vinyl-containing silanes: trichlorovinylsilane (TCVS, Aldrich, St. Louis, MO), and allyldimethylchlorosilane (ADCS, Alfa Aesar, Ward Hill, MA). In each case, bare silica microspheres were suspended in a freshly-prepared 5% (v/v) solution of either TCVS or ADCS in dry chloroform at room temperature for 3 h. The microspheres were then washed three times each with dry chloroform, dry ethanol and HPLC-grade H_2O (the residual ethanol facilitates H_2O wetting of the now-hydrophobic surface) [16]. The silanized microspheres were dried overnight at 110 °C, and stored desiccated under inert gas in the dark to prevent oxidation of the vinyl groups.

Silicon wafer disks (1.0 cm^2, WaferNet, San Jose, CA) were used as the substrate for enzyme-linked immunosorbent assay (ELISA) experiments. Wafers were washed as described above, and then modified with TCVS by a vapor deposition procedure [17]. Clean, dry wafers were placed in a vapor-phase reactor to which flowing dry nitrogen was introduced for 1 h. The nitrogen stream was then passed through a reservoir containing liquid TCVS at 25 °C to entrain the silane vapor. After about two hours, the TCVS had completely evaporated (leaving a small amount of non-volatile residue), and the nitrogen was allowed to flow for another hour to purge the reactor. The TCVS-modified wafers were stored desiccated in the dark under inert gas.

C.2.3 Surface coating with F108 and EGAP-NTA triblocks

Triblocks were covalently attached to the silanized microsphere surfaces according to methods described by McPherson *et al*. [16] and Park *et al*. [18], in which PEO-PPO-PEO triblocks were adsorbed on the hydrophobic surfaces produced by reaction of metal oxides with a vinyl silane, then subjected to γ -irradiation. Absorption of radiation or interaction with

water-derived radicals forms surface-bound free radicals, which attack the neighboring adsorbed PPO block, forming covalent bonds between the surface and polymer [16].

TCVS-treated microspheres were coated by overnight incubation with a 0.50% solution of either F108 or EGAP-NTA triblock in PBS (the ADCS-treated samples were coated with F108 only). After incubation, some of the samples were washed three times with PBS prior to γ-irradiation; the remaining samples were kept in the 0.50% triblock coating solution. The surfactant-coated microspheres were irradiated to a dose of 0.3 Mrad by a ^{60}Co source, then washed twice with PBS. Un-irradiated triblock layers (i.e. F108/EGAP-NTA bound to the vinyl-rich microsphere surface by hydrophobic association only) served as controls for layer stability tests. The stability of the triblock/surface association was evaluated by incubation of coated microspheres with 5% SDS in PBS for 1 h to dislocate non-covalently bound surfactant. Zeta potential measurement was used to evaluate the stability of the triblock coating.

C.2.4 Individual and sequential protein adsorption

Silanized, triblock-coated or uncoated microspheres (10% w/v) were incubated for 4 h with PBS or with PBS containing 10 mg/mL nisin or 10 mg/mL fibrinogen, then rinsed with 2 volumes of PBS. The rinsed microsphere suspensions were further incubated with PBS or with fibrinogen in PBS for 4 h. All microsphere samples were then rinsed twice with PBS to remove loosely-bound protein.

C.2.5 Zeta potential analysis

A 10 μL aliquot of a 10% microsphere suspension was diluted into 2 mL of 1 mM KCl (pH 7.55) in a disposable polystyrene cuvette. The diluted sample was then analyzed for 5 cycles of 30 recordings/cycle, using the phase analysis-light scattering (PALS) mode of a ZetaPALS system (Brookhaven Instruments Corp., Holtsville, NY).

C.2.6 Enzyme-linked immunosorbent assay (ELISA)

Flat, TCVS-modified silicon wafers were incubated with F108 (10 mg/mL in PBS) for 4 h, and irradiated in the presence of the F108 coating solution as described above. Wafers with and without F108 coatings were incubated with PBS or a 0.05 mg/mL solution of commercial nisin (Sigma-Aldrich N5764) in PBS for 4 h. F108-coated and uncoated wafers, with and without adsorbed nisin, were then transferred to the bottoms of BSA-blocked wells in a polystyrene micro-test plate. Each sample was covered with fibrinogen (0.01 mg/mL in PBS) for 1 h, and then rinsed three times with PBS. Samples were incubated for 1 h with the HRP-labeled anti-fibrinogen antibody and rinsed again according to manufacturer's instructions (with the exception that HEPES-buffered saline with BSA was prepared in the absence of Tween 20 to reduce the possibility of elution of loosely-held fibrinogen). Bound HRP was quantified by reaction with *o*-phenylenediamine and H_2O_2 for 20 min. The reaction was quenched with sulfuric acid, and the absorbance of each sample (490 nm) used to calculate the adsorbed amount of fibrinogen.

C.3 Results and Discussion

C.3.1 Silanization with TCVS vs. ADCS

McPherson *et al*. [16] and Park *et al*. [18] described the covalent binding of PEO-PPO-PEO triblocks to TCVS-modified glass, metal and pyrolytic carbon surfaces by γ-irradiation. In the present study, triblock immobilization on layers formed by the monofunctional silane ADCS was also evaluated; this reagent cannot polymerize, and thus was expected to produce a smoother, more uniform layer for triblock coating than TCVS [19]. Representative zeta potential measurements of uncoated and F108-coated TCVS/ADCS-treated microsphere suspensions which were not γ-irradiated are shown in Figure C.1. Surfaces treated with TCVS consistently

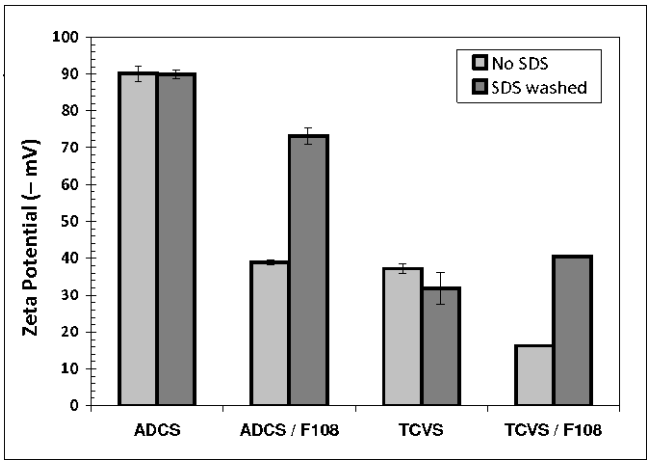

Figure C.1. Effect of SDS washing on measured zeta potential of uncoated and F108-coated microspheres silanized with TCVS or ADCS. These samples were not subjected to γ - irradiation.

showed less negative zeta potentials than their ADCS counterparts. We ascribe this effect to the thicker layers typically produced by polymerization of the trifunctional silane TCVS. Although coating with F108 could be expected to mask variations in surface charge (zeta potential) caused by due differences in silane layer thickness, this effect was not observed

(Figure C.1). It is possible that the TCVS treatment leaves a relatively rough surface, which better accommodates a dense packing of the triblocks. But whether silanized by TCVS or ADCS, all un-irradiated surfaces coated with F108 exhibited a significantly more negative zeta potential upon SDS challenge, to an extent consistent with near-complete removal of the F108. The zeta potential of uncoated, silanized microspheres remained largely unchanged following treatment with SDS; this is an expected result for reversible binding of SDS on a stable surface layer.

Representative zeta potentials for uncoated and F108-coated microsphere suspensions that were subjected to γ-irradiation are shown in Figure C.2. The F108-coated microsphere suspensions were

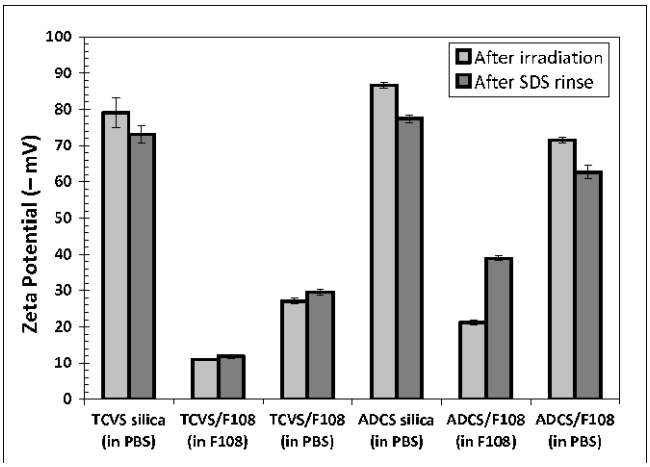

Figure C.2. Effect of SDS washing on measured zeta potential of uncoated and F108-coated microspheres silanized with TCVS or ADCS, and subjected to γ -irradiation. Microspheres were irradiated either in PBS ("washed") or in the F108 coating solution ("unwashed").

γ -irradiated either in PBS after washing three times with the same buffer ("washed"), or in the presence of the 0.50% F108 solution used for coating ("unwashed"). The washed samples (i.e. those irradiated in PBS) had a consistently more negative zeta potential than their unwashed counterparts, regardless of the silane used for pretreatment. This suggests that irradiation of

silanized surfaces in the presence of F108 produced a denser, more uniform triblock coating. Moreover, the TCVS-silica samples irradiated in F108 showed essentially no significant change in zeta potential upon challenge with SDS, while those pretreated with ADCS showed a substantial negative shift upon challenge with SDS. As with the unirradiated samples (Figure C.1), the zeta potential of the uncoated samples remained largely unchanged upon treatment with SDS, consistent with reversible SDS binding.

The zeta potential for uncoated TCVS-treated microspheres (about -37 mV; Figure C.1) became significantly more negative (about -79 mV) after γ -irradiation. McPherson *et al*. attribute this increase in negative surface charge density to radiation-induced loss of the vinyl-rich surface layer itself, exposing the silica substrate. However, the zeta potential of the irradiated uncoated TCVS samples was more negative than that of unmodified silica itself (-70 mV, data not shown), yet stable coatings were also formed in the presence of F108. We speculate that dissolved O_2 contributes to the radiation-induced oxidation of the vinyl C=C bonds to form ionizable, hydrophilic species.

The results of Figures C.1 and C.2 indicate that γ-irradiation of TCVS-treated, F108-coated surfaces in the presence of the F108 coating solution produced denser, more stable F108 layers than washed or ADCS-treated surfaces. Based on these results, all triblock coatings for further individual protein and sequential adsorption experiments were produced by TCVS treatment and γ -irradiation in the triblock coating solution.

C.3.2 Triblock layer stability

Figure C.3 shows the zeta potentials of TCVS-treated microspheres coated with EGAP-NTA, with and without stabilization by γ -irradiation in the presence of 0.50% EGAP-NTA in PBS. For comparison, the analogous data for F108-coated microspheres (Figures C.1

and C.2) have been redrawn in Figure C.3. The more negative zeta potential recorded for microspheres coated with

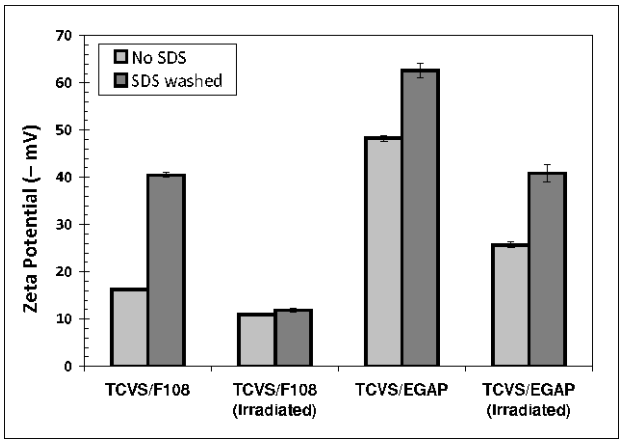

Figure C.3. Effect of γ -irradiation on the resistance of F108 and EGAP-NTA layers to elution by SDS, as determined by zeta potential of TCVS-treated, triblock-coated microspheres. Microspheres were γ -irradiated in the triblock coating solution in each case.

EGAP-NTA relative to F108 is attributed to the highly anionic NTA end group. But while γ -stabilization of the EGAP-NTA layer was accompanied by a change in zeta potential to a less negative value, these layers appeared to remain somewhat elutable by SDS. Experimentally, the microsphere suspensions coated with EGAP-NTA tended to resist pellet formation upon centrifugation. Following SDS challenge, the efficient washing with PBS was hindered by attempts to minimize bead loss, and so the observed high negative surface charge may be due in part to residual negatively-charged SDS near the interface.

C.3.3 Individual protein and sequential adsorption of nisin and fibrinogen

Uncoated, F108-coated and EGAP-NTA-coated microspheres were incubated with nisin or with fibrinogen in independent experiments. Microsphere samples were also incubated with nisin, rinsed and then incubated with fibrinogen (sequential adsorption). Figure C.4 shows zeta potential changes due to protein adsorption on uncoated surfaces. The surface charge of uncoated

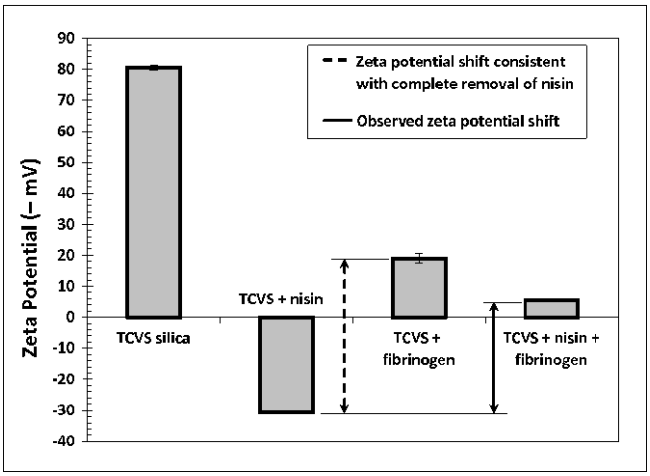

Figure C.4. Zeta potential detection of protein adsorption to uncoated, TCVS-modified and irradiated microspheres incubated with nisin alone, with fibrinogen alone, and incubated sequentially with nisin followed by fibrinogen. Microspheres were γ -irradiated in PBS (i.e. no triblocks adsorbed) prior to protein contact.

microspheres became positive (+30 mV) after nisin contact, consistent with adsorption of the cationic polypeptide at the surface. The high negative charge density of the uncoated microspheres remained negative, but was masked appreciably after incubation with fibrinogen, consistent with fibrinogen adsorption at the silanized microsphere surface. Fibrinogen has an isolectric point between 5.1 and 6.3, and therefore has a net negative charge at neutral pH.

The difference between the second and third bars in Figure C.4 (i.e. zeta potential of nisin- and fibrinogen-contacted surfaces) quantifies a shift in potential that would be consistent with the complete replacement of nisin on a TCVS-modified surface by fibrinogen. The difference between the second and fourth bars in Figure C.4 (adsorption of nisin vs. sequential adsorption of nisin and fibrinogen) is the actual (observed) shift in zeta potential. It is instructive to compare the observed shift to the maximum possible value. The positive charge density produced by incubation with nisin alone became substantially negative after subsequent incubation with fibrinogen, indicating significant removal of adsorbed nisin. In

particular, contact with fibrinogen produced a shift in zeta potential equivalent to 73% of that associated with the complete removal of nisin.

Figures C.5 and C.6 show zeta potential changes due to protein adsorption on F108- and EGAP-NTA-coated surfaces. Similar to the results just discussed, these results show that the observed surface charge density became positive after nisin contact, indicative of nisin adsorption at these PEO layers. Zeta potentials recorded after incubation with fibrinogen are in each case consistent with good fibrinogen repulsion by each type of PEO layer. The very small shift in zeta potential to a more negative value after fibrinogen contact observed with the F108 layer (Figure C.5) can probably be attributed to non-uniformities in the triblock layer [15], giving rise to regions of unprotected hydrophobic silica that allow unhindered adsorption of fibrinogen.

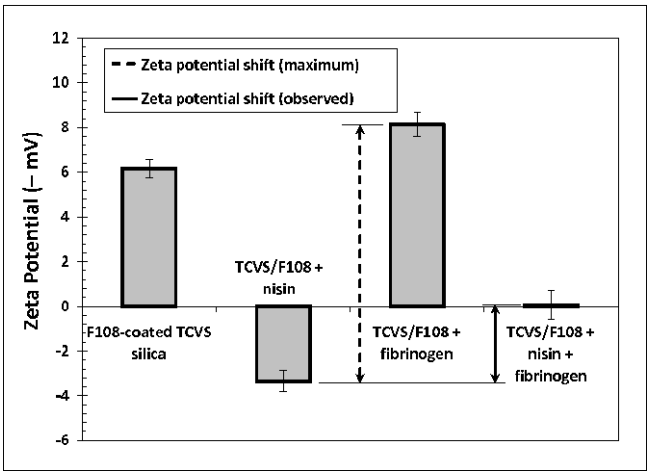

Figure C.5. Zeta potential detection of protein adsorption to F108-coated, TCVS-modified microspheres incubated with nisin alone, with fibrinogen alone, and incubated sequentially with nisin followed by fibrinogen. Microspheres were γ -irradiated in F108 coating solution prior to protein contact.

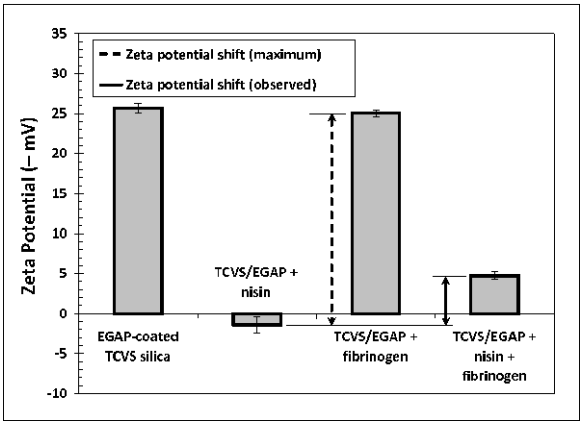

Figure C.6. Zeta potential detection of protein adsorption to EGAP-NTA-coated, TCVS-modified microspheres incubated with nisin alone, with fibrinogen alone, and incubated sequentially with nisin followed by fibrinogen. Microspheres were □-irradiated in EGAP-NTA coating solution prior to protein contact.

The presence of nisin entrapped within immobilized PEO was validated in related experiments, using X-ray photoelectron spectroscopy (XPS). In those experiments, silicon wafers were made hydrophobic by treatment with octadecyltrimethoxysilane in ethanol to form a C_{18} surface coating. Triblocks with a polybutadiene centerblock (PEO-PBD-PEO) were adsorbed on these C_{18} surfaces and immobilized by γ -irradiation as described above. In this system, the triblocks themselves contain the activated double-bonds that covalently bond with the otherwise inert C_{18}-modified surface [16]. After washing the irradiated surfaces to remove loosely-bound triblocks, the PEO brush layers were challenged with nisin in PBS, as described above, with reference to microsphere samples. After extensive washing with buffer and water to remove excess nisin, the wafers were dried under vacuum and examined by XPS (Thermo-Fisher ESCALAB 250) equipped with a monochromatic Al Kα X-ray source (1486.6 eV). Survey and high-resolution C_{1s}, N_{1s}, O_{1s}, and $S_{2s/2p}$ spectra were recorded at a take-off angle of 0°. The high-resolution peaks were quantified using Shirley background removal and the manufacturer's sensitivity factors. The C_{1s} peak was deconvoluted using the supplied peak-

fitting software. A distinct C_{1s} peak was observed at 286.3 eV on the triblock-coated, irradiated surface; this binding energy corresponds to polyether C-O bonds and is consistent with a stable PEO coating. Following incubation with nisin and several washes, the PEO-coated surfaces exhibited a strong N_{1s} peak and small $S_{2s/2p}$ peaks, indicating the presence of nisin protein at the surface PEO layer. The calculated atom% ratio of N_{1s}:S_{2p} was 5.6 (data not shown), consistent with a N/S ratio of 6.0 calculated from the known composition of nisin. Although taken from a different triblock coating, these XPS results indicate that nisin can be entrapped within immobilized PEO.

Both Figures C.5 and C.6 show that the positive charge density evident after incubation with nisin alone became negative again following subsequent incubation with fibrinogen, indicating some removal of entrapped nisin in the presence of fibrinogen. But in contrast to uncoated silica, the sequential contact with fibrinogen in these cases produced a smaller shift in zeta potential, only 30% of that consistent with the complete removal of nisin at the F108 layer, and 23% of that consistent with the complete removal of nisin at the EGAP-NTA layer.

These data indicate that nisin integrates into covalently stabilized, fibrinogen-repellent PEO layers. Moreover, we observed nisin to be substantially more resistant to elution by fibrinogen when entrapped in PEO than when simply adsorbed at an uncoated surface. If present at the interface in multilayer quantities, we should expect nisin located nearer the chain ends to be less resistant to elution than nisin located deeper within the PEO [13]. Thus the sequential adsorption results can be taken as consistent with the outermost nisin molecules being eluted while PEO segments extending beyond the level of entrapped nisin retain their steric repulsive character. On the other hand, the results shown in Figures C.4-6 do not preclude the possibility of fibrinogen adsorption, presumably at regions of the nisin-loaded

PEO layer where electrostatic interactions could be important and the steric repulsive capability of the PEO could be compromised, due to the presence of the peptide.

Any preferential location of a procoagulant protein such as fibrinogen at a peptide-loaded PEO layer would significantly reduce the viability of a medical device coating based on this approach. Figure C.7 shows results of ELISA experiments performed with uncoated and F108-coated silica samples, in the presence and absence of adsorbed nisin. These results suggest that the presence of nisin in the PEO layer evoked a fibrinogen loading that is not substantially greater than with PEO alone. However, the presence of fibrinogen was apparent on each of the F108-coated surfaces tested. The fibrinogen detected at these surfaces may be explained by the reasonable assumption of PEO layer non-uniformities that compromise fibrinogen repulsion, but may also be an outcome of the ELISA technique itself, including difficulties associated with ensuring the absence of nonspecific adsorption by HRP-labeled anti-fibrinogen. Questions surrounding fibrinogen adsorption in this context warrant further investigation with a more direct, surface analytical approach, and will contribute to the subject of a future report.

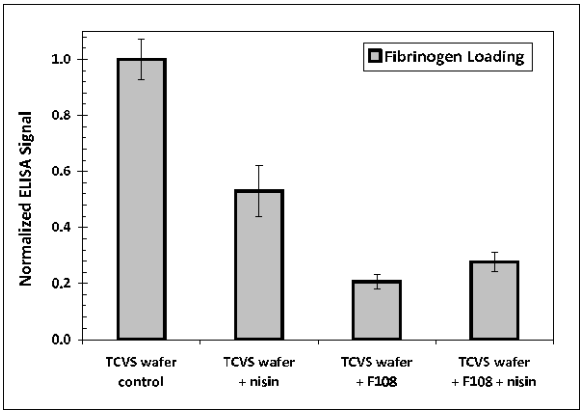

Figure C.7. Relative fibrinogen adsorption on uncoated and F108-coated TCVS-modified surfaces in the presence and absence of adsorbed nisin. Uncoated surfaces were γ -irradiated in PBS prior to protein contact; the F108-coated surfaces were γ -irradiated in F108 coating solution. Values shown are normalized to the response of fibrinogen adsorbed to the uncoated, TCVS-treated silica.

C.4 Summary

Hydroxyl- and nitrilotriacetic acid-terminated PEO-PPO-PEO triblock coatings adsorbed on silica surfaces modified with TCVS and γ -irradiated in the presence of triblock solution were resistant to elution by SDS and showed good fibrinogen repulsion. Nisin adsorption to these PEO layers was detected by zeta potential measurements. Nisin appeared substantially more resistant to elution in the presence of fibrinogen when entrapped in PEO than when adsorbed at an uncoated surface. Tentatively, the sequential adsorption results reported here are consistent with the partial elution of nisin in the presence of fibrinogen, but retention of the steric repulsive quality of the layer.

C.5 Acknowledgments

This work was supported in part by the National Institute of Diabetes and Digestive and Kidney Diseases (grant no. 2 R44 DK 072560-02). The authors would like to thank the staff at Allvivo Vascular Inc. for synthesizing the EGAP-NTA used in this work, and Dr. Tom Shellhammer of OSU for use of his ZetaPALS instrument.

C.6 References

[1] D.C. Dugdale, P.G. Ramsey, Am. J. Med. 89 (1990) 137.

[2] I. Raad, J. Narro, A. Khan, J. Tarrand, S. Vartivarian, G.P. Bodey, Eur. J. Clin. Microbiol. Infect. Dis. 11 (1992) 675.

[3] I. Raad, G.P. Bodey, Clin. Infect. Dis. 15 (1992) 197.

[4] C.K. Bower, M.K. Bothwell, J. McGuire, Colloids Surf. B: Biointerfaces 22 (2001) 259.

[5] C.K. Bower, J.E. Parker, A.Z.Higgins, M.E. Oest, J.T. Wilson, B.A. Valentine, M.K. Bothwell, J. McGuire, Colloids Surf. B: Biointerfaces 25 (2002) 81.

[6] Y.-C. Tai, P. Joshi, J. McGuire, J.A. Neff, J. Colloid Interface Sci. 322 (2008) 112.

[7] Y.-C. Tai, J. McGuire, J.A. Neff, J. Colloid Interface Sci. 322 (2008) 104.

[8] M. Malmsten, K. Emoto, J.M. Van Alstine, J. Colloid Interface Sci. 202 (1998) 507.

[9] M. Rovira-Bru, F. Giralt, Y. Cohen, J. Colloid Interface Sci. 235 (2001) 70.

[10] J.G. Archambault, J.L. Brash, Colloids Surf. B. Biointerfaces. 33 (2004) 111.

[11] A. Halperin, Langmuir. 15 (1999) 2525.

[12] S.R. Sheth, D. Leckband, Proc. Natl. Acad. Sci. USA. 94 (1997) 8399.

[13] F. Fang, J. Satulovsky, I. Szleifer, Biophys. J. 89 (2005) 1516.

[14] L.D. Unsworth, H. Sheardown, J.L. Brash, Langmuir. 24 (2008) 1924.

[15] P. Katira, A. Agarwal, H. Hess, Adv. Mater. 20 (2008) 1-6.

[16] T.B. McPherson, H.S. Shim, K. Park, J. Biomed. Mater. Res. 38 (1997) 289.

[17] K.C. Popat, R.W. Johnson, T.A. Desai, Surf. Coatings Technol. 154 (2002) 253.

[18] K. Park, H.S. Shim, M.K. Dewanjee, N.L. Eigler, J. Biomater. Sci. Polym. Ed. 11 (2000) 1121.

[19] S. Rajam, C.-C. Ho, J. Membr. Sci. 281 (2006) 211.

APPENDIX D

QUANTIFYING NISIN ADSORPTION BEHAVIOR AT PENDANT PEO LAYERS

Justen K. Dill, Julie A. Auxier, Karl F. Schilke and Joseph McGuire*

School of Chemical, Biological and Environmental Engineering
Oregon State University, Corvallis, OR 97331

* Corresponding Author:

Joseph McGuire
School of Chemical, Biological and Environmental Engineering
Oregon State University
103 Gleeson Hall
Corvallis, OR 97331-2702

Tel: 541-737-6306
Fax: 541-737-4600
Email: *joseph.mcguire@oregonstate.edu*

J. Colloid Interface Sci., submitted October 2012, in review

Abstract

The antimicrobial peptide nisin shows potent activity against Gram-positive bacteria including the most prevalent implant-associated pathogens. Its mechanism of action minimizes the opportunity for the rise of resistant bacteria and it does not appear to be toxic to humans, suggesting good potential for its use in antibacterial coatings for selected medical devices. A more quantitative understanding of nisin loading and release from polyethylene oxide (PEO) brush layers will inform new strategies for drug storage and delivery, and in this work optical waveguide lightmode spectroscopy was used to record changes in adsorbed mass during cyclic adsorption-elution experiments with nisin, at uncoated and PEO-coated surfaces. PEO layers were prepared by radiolytic grafting of Pluronic® surfactant F108 or F68 to silanized silica surfaces, producing long- or short-chain PEO layers, respectively. Kinetic patterns were interpreted with reference to a model accounting for history-dependent adsorption, in order to evaluate rate constants for nisin adsorption and desorption, as well as the effect of pendant PEO on the lateral clustering behavior of nisin. Nisin adsorption was observed at the uncoated and F108-coated surfaces, but not at the F68-coated surfaces. Nisin showed greater resistance to elution by peptide-free buffer at the uncoated surface, and lateral rearrangement and clustering of adsorbed nisin was apparent only at the uncoated surface. We conclude peptide entrapment at the F108-coated surface is governed by a hydrophobic inner region of the PEO brush layer that is not sufficient for nisin entrapment in the case of the shorter PEO chains of the F68-coated surface.

Keywords: adsorption kinetics, history dependent model, nisin, PEO brush, peptide entrapment

D.1 Introduction

Nisin is a small (3.4 kDa) cationic, amphiphilic peptide that is an effective inhibitor of Gram-positive bacteria[29]. Its potential use in anti-infective coating strategies has motivated interest in its adsorption and function at biomaterial interfaces. We have described nisin adsorption and various aspects of its behavior at PEO-coated surfaces through ellipsometry[30], circular dichroism and assays of antibacterial activity[31], zeta potential[32], and TOF-SIMS[24].

In this paper, optical waveguide lightmode spectroscopy (OWLS) was used to record changes in adsorbed mass during cyclic adsorption-elution experiments with nisin, at PEO layers prepared by covalent stabilization of Pluronic® surfactant F108 or F68 to silanized silica surfaces, producing long- or short-chain PEO layers, respectively. Kinetic patterns were interpreted with reference to a model accounting for history-dependent adsorption[33].

D.2 Materials and Methods

D.2.1 Solution preparation.

Nisin (3510 Da) was obtained from Prime Pharma (Batch number 20050810, Gordons Bay, South Africa) and dissolved in 10 mM monobasic phosphate buffer (10 mM monobasic sodium phosphate, 150 mM sodium chloride). The pH was adjusted to 7.4 by dilution with dibasic phosphate buffer (10 mM dibasic sodium phosphate, 150 mM sodium chloride) to bring the final nisin concentration to 0.5 mg/mL. The solution was stirred overnight in a 37 ˚C incubator. Plasminogen-free human fibrinogen (340 kDa, 1 mg/mL, Sigma-Aldrich) was dissolved in phosphate buffered saline (PBS, 10 mM sodium phosphate buffer, 150 mM NaCl, pH 7.4) as needed. Prior to use, all protein solutions were drawn into sterile, disposable syringes and degassed for 1 h at 700 torr vacuum. All protein free PBS solutions were degassed in a sterile, disposable syringe at 700 torr vacuum for 4 h. The Pluronic® surfactants F108 and F68 were obtained from BASF (Mount Olive, NJ) and dissolved in PBS, each at 5% (w/v) as needed. All water used was HPLC grade.

D.2.2 Surface modification.

OW 2400 waveguide sensors for use with OWLS instrumentation were purchased from MicroVacuum (Budapest, Hungary). A thin film of silica dioxide was applied by the manufacturer prior to purchase. Sensor cleaning consisted of submersion in chromosulfuric acid (Acros Organics, NJ) for 10 min, rinsing with HPLC grade water, and blow drying with dry nitrogen. Surface silanization was performed via vapor deposition with trichlorovinylsilane (TCVS, TCI America, Portland, OR). Silanization was carried out in a sealed vessel using dry argon as the carrier gas [34]. Cleaned OWLS sensors were arranged on the sample stage with the waveguides facing up. Dry argon was allowed to flow through the vapor deposition unit to equilibrate the internal environment and purge any atmospheric

moisture. A 200 µL aliquot of TCVS was injected into the injection well and argon flow directed through the well to transport silane vapors into the main chamber. After 1 h, another 200 µL aliquot of TCVS was injected into the well. Argon flow was continued for an additional hour before bypassing the injection well. Argon was then passed through the main chamber for an additional 20 min to purge any unreacted silane vapors from the system.

Silanized waveguides were cured at 150 ˚C for 20 min to stabilize the newly formed vinyl layer. Each silanized and cured waveguide was incubated for a minimum of 12 h in a 1.5 mL microcentrifuge tube containing the desired triblock solution. After incubation, these tubes were exposed to γ-radiation from a ^{60}Co source (Oregon State University Radiation Center) for a total dose of 0.3 Mrad (6.5 hours) to achieve polymer grafting [35]. Sensors were then removed from incubation tubes, rinsed with PBS, dried with nitrogen, and stored in dry nitrogen filled microcentrifuge tubes until needed.

D.2.3 OWLS measurements.

OWLS waveguides (with or without surface modifications) were immersed in PBS overnight prior to use in order to equilibrate their surface with the buffer [36]. The waveguide was then removed from solution and immediately installed in the OWLS flow cell (total volume 4.8 µL). Experiments were carried out in an OWLS 210 instrument controlled with BioSense 2.6 software (MicroVacuum, Budapest, Hungary). A Rheodyne manual sample injector (IDEX, Oak Harbor, WA) was used to inject protein samples through a flow loop (PEEK tubing, 2.3 mL approximate volume) to the OWLS flow cell. The flow rate was maintained at 50 µL/min in all experiments to ensure an injection residence time of at least 30 min in the flow cell. As refractive index measurements are highly sensitive to temperature variations, flow cell temperature was maintained at 20 ˚C by an internal OWLS TC heater/cooler unit. Incident angle scans were performed from -5˚ to 5˚ at a step size of 0.01˚.

All four peaks were measured (the characteristic transverse electric (TE) and transverse magnetic (TM) peaks) to determine the relative refractive index of the surface adlayer. The OWLS instrument allows 4-10 peak scans per minute (depending on scanning speeds, peak ranges, and number of peaks used), which resulted in about 6 s being needed for determination of a single data point. Adsorbed mass versus time data was calculated from changes in the refractive index of the adlayer, applying the assumption that refractive index changes linearly with protein concentration [37].

D.2.4 Adsorption kinetics.

Cyclic, adsorption-elution experiments were performed with each triblock surfactant (5% w/v), fibrinogen (1 mg/mL), or nisin (0.5 mg/mL). In each case, once loaded into the injection loop, about 6 mL of solution was passed through the loop to purge any remaining equilibration buffer. In the case of the triblocks, adsorption was performed for 30 min on a TCVS-treated sensor, immediately followed by a 30 min rinse with protein-free buffer in each cycle. In the case of fibrinogen, adsorption was performed for 10 min on triblock-coated and uncoated (TCVS-treated) sensors for the purpose of confirming the presence of protein-repellent PEO layers after grafting. Nisin adsorption was performed for 30 min, immediately followed by a 30 min rinse with protein-free buffer on uncoated, F108-coated, and F68-coated surfaces. This process was repeated two times during the course of one experiment.

D.3 Results and Discussion

D.3.1 Triblock adsorption.

The Pluronic® surfactants F108 and F68 were adsorbed to silanized OWLS waveguides prior to covalent immobilization (while immersed in 5% triblock solution) through γ-irradiation. Figure D.1 shows representative results of adsorption experiments performed on these waveguide sensors to confirm triblock association with the hydrophobic surface. Each triblock adsorbed rapidly to the hydrophobic surface of the waveguide, and adsorbed mass remained fairly constant over the 30 min adsorption cycle. Taking the plateau amounts of adsorbed triblock shown in Figure D.1 as an upper limit to estimate the PEO chain density at each surface, we would record 0.25 and 0.34 chains/nm^2 in the case of F108 and F68, respectively. Formation of a less dense brush layer in the case of F108 is consistent with its longer PEO chains (about 141 repeat units vs. 80 for F68) as well as the larger footprint afforded by its PPO center block (about 44 repeat units vs. 27 for F68). This would constitute only a rough estimate, however, as it is difficult to know the orientation and association state of triblocks at the time of γ-irradiation. Instead, we verified adoption of a brush configuration in each case by fibrinogen repulsion (Figure D.2). PEO brush layers with good steric-repulsive function are expected to form at chain densities greater than about 0.2 chains/nm^2 [38]. The nonfouling character of the PEO layers formed in this work was clearly evident upon introduction of human fibrinogen to uncoated and PEO-coated waveguide sensors (Figure D.2).

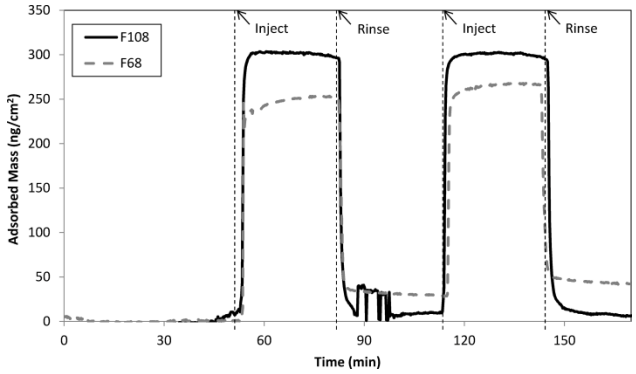

Figure D.1. Adsorption patterns recorded after exposure of TCVS-treated OWLS waveguides to a 5% F108 or F68 solution (in PBS), followed by elution in surfactant-free PBS.

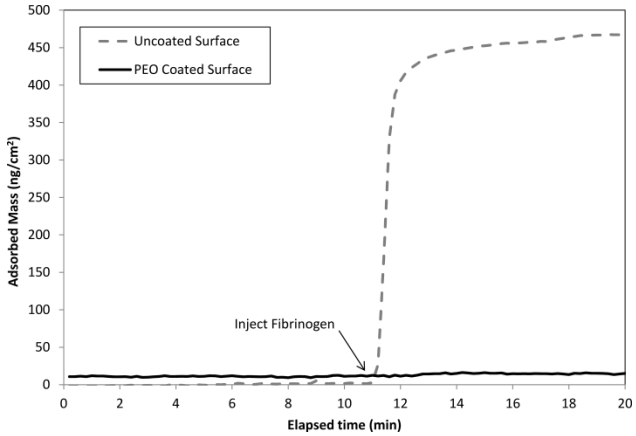

Figure D.2. Representative plot of fibrinogen adsorption at an uncoated and PEO-coated surface.

D.3.2 Nisin adsorption.

Representative results for nisin adsorption at uncoated, F108-coated, and F68-coated waveguides is shown in Figure D.3. The greatest extent of adsorption and greatest resistance to elution was recorded on the uncoated surface. While nisin adsorbed to the F108-coated surface with good affinity, it was substantially less resistant to elution. No appreciable adsorption of nisin was recorded at the F68 layer.

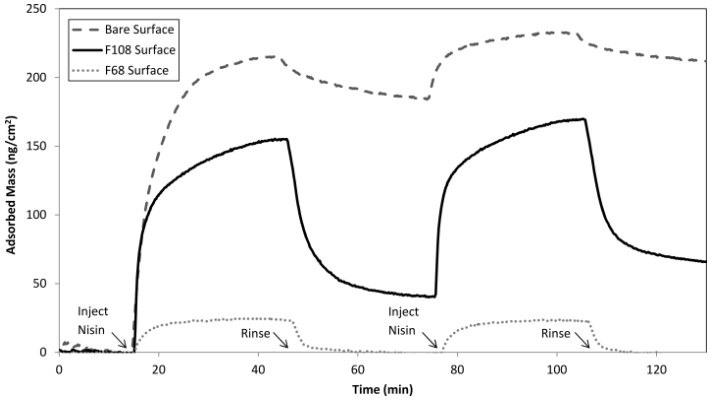

Figure D.3. Nisin adsorption at uncoated, F108-coated, and F68-coated waveguides.

While nisin apparently entered the F68 brush during the adsorption step, association with the surface and/or the surrounding PEO chains was not sufficient to retain the peptide during the rinse step. We note that while preparation of fibrinogen-repellent PEO layers based on F108 triblocks was straightforward, preparation of such layers based on F68 triblocks was not routinely successful. As a result nisin adsorption was recorded at F68 layers in some experiments, but fibrinogen adsorption was recorded in such cases as well. Analysis of these outcomes, to be discussed in a separate report, suggests that any nisin adsorption at an F68 layer is attributable to non-uniform brush formation, allowing direct contact and adsorption of the peptide at uncoated defect regions on the surface.

D.3.3 Visual inspection of history-dependent behavior.

At a given surface loading, the rate of adsorption will depend on the formation history of the adsorbed layer. For example, adsorbed protein may rearrange laterally or "cluster" at the surface to form more ordered domains, in this way increasing the interfacial area available for incoming protein to adsorb without overlapping those previously adsorbed [33]. Such history dependent adsorption behavior has been recorded for a number of proteins at solid surfaces [30, 39-41]. The curves in Figure D.4a show that the initial adsorption rate during the

second cycle was considerably greater than the adsorption rate at the uncoated hydrophobic surface, at the same surface coverage as during the first cycle. Based on its solution dimensions, a monolayer of nisin adsorbed "end-on" (occupying about 4 nm^2/molecule) would be consistent with an adsorbed mass of about 145 ng/cm^2 [42]. It is thus reasonable to suspect that an outer layer of adsorbed nisin, bound by its association with nisin molecules that are adsorbed in the primary layer, may participate in the lateral clustering giving rise to history dependent behavior at the uncoated surface.

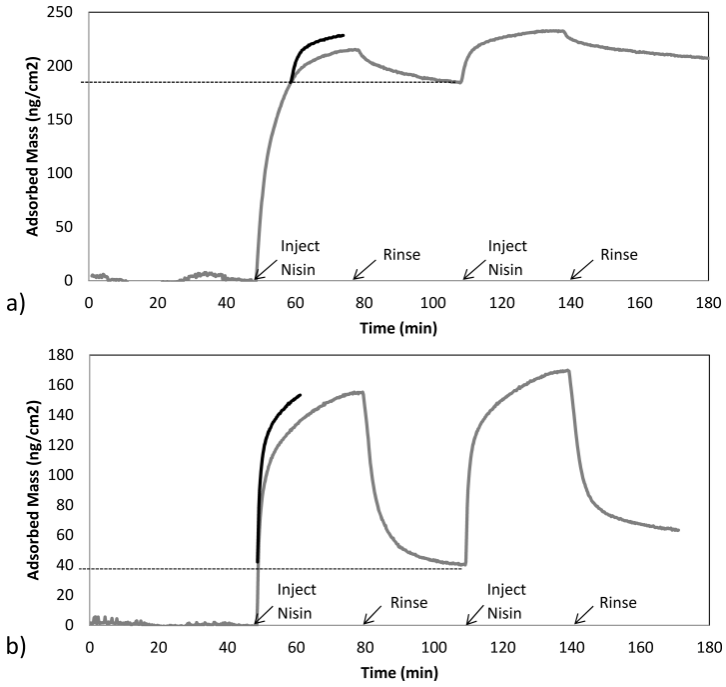

Figure D.4. Nisin adsorption at (a) uncoated and (b) F108-coated waveguides. In each panel, the initial rate data in the second cycle is shifted back in order to allow comparison of adsorption rates at equal surface coverages in each cycle.

On the other hand the initial adsorption rate during the second cycle was nearly identical to the adsorption rate at the same surface coverage during the first cycle in the case of adsorption to the F108 layer (Figure D.4b). This lack of history dependence might suggest

inhibition of nisin clustering owing to the presence of the PEO chains. However theoretical and experimental evidence suggests that below the hydrophilic outer region of a PEO brush there exists a hydrophobic region that is favorable for protein adsorption [43, 44]. At the high chain concentrations consistent with brush formation, the specific configuration of the PEO that enables hydrophilic interaction with water becomes disrupted, rendering the pendant chains less soluble (or even insoluble) in water [45-47]. Recently, Lee *et al*. demonstrated that PEO chains are not hydrophilic when they are arranged in the brush configuration [48]. They found however that the brush layer hydrophobicity is not sufficient to overcome the PEO conformational entropy, consequently preventing collapse and preserving the widely observed steric-repulsive character.

The presence or absence of history dependent adsorption might indicate different adsorption mechanisms at play in each instance. Adsorption to the F108 layer may be best characterized by entrapment within the hydrophobic PEO phase, without contacting the underlying surface. Beyond some threshold concentration of peptide within this phase, its attractiveness for further protein adsorption may become compromised as interactions among PEO chains are disrupted or otherwise give way to PEO-peptide interactions. Peptides arriving after this threshold is reached could well be highly elutable. Certainly the lack of stable nisin adsorption recorded at the F68 layer also points to a lack of stable association between nisin and the underlying surface. We suggest nisin entrapment involves its location within the hydrophobic region of the immobilized PEO layer. While no evidence of stable association between nisin and the hydrophobic region of the F68 layer was recorded, this may be owing to the relatively short PEO chain length afforded by immobilized F68.

D.3.4 Comparison to a model.

When a surface is exposed to a protein solution and the adsorption is kinetically limited, the rate of adsorption can be described by

$$\frac{d\Gamma}{dt} = k_a e^{\frac{-\bar{U}_s(\Gamma)}{kT}} C_b \Phi - \sum_i k_{d,i} \Gamma_i \qquad [1]$$

where Γ is the adsorbed mass, t is time, k_a is the intrinsic adsorption rate constant, C_b is the bulk concentration of the adsorbing molecules in solution, and $k_{d,i}$ and Γ_i are the desorption rate constant and the density of adsorbed molecules in the i^{th} adsorption state [33]. Φ is the cavity function, dependent on different factors but conveniently considered to be the fraction of the surface where a molecule can adsorb without overlapping a previously adsorbed molecule. The term, $e^{\frac{-\bar{U}_s(\Gamma)}{kT}}$, accounts for the influence of protein surface concentration on the adsorption rate, where $-\bar{U}_s(\Gamma)$ is an average energy for the first adsorbates, k is the Boltzmann constant, and T is temperature. Multiplying through by $\left(\frac{e^{\frac{-\bar{U}_s(0)}{kT}}}{e^{\frac{-\bar{U}_s(0)}{kT}}} \right)$,

$$\frac{d\Gamma}{dt} = kC\Phi' - \sum_i k_{d,i} \Gamma_i \qquad [2]$$

where $kC = k_a e^{\frac{-\bar{U}_s(0)}{kT}} C_b$, which can be experimentally determined during the first adsorption cycle on an empty surface (i.e., at $\Gamma = 0$), and $\Phi' = \Phi \left(\frac{e^{\frac{-\bar{U}_s(\Gamma)}{kT}}}{e^{\frac{-\bar{U}_s(0)}{kT}}} \right)$.

The data of Figure D.3 can be replotted as adsorption rate vs. adsorbed mass to determine the kinetic parameters in Eq. [2]. At $\Gamma = 0$, the modified cavity function, Φ', is equal to 1, and Eq. [2] can be written as $\left.\frac{d\Gamma}{dt}\right|_{\Gamma=0} = kC$. Thus the *y*-intercept of the best fit lines in Figure D.5 may be used to determine an effective kC for each surface.

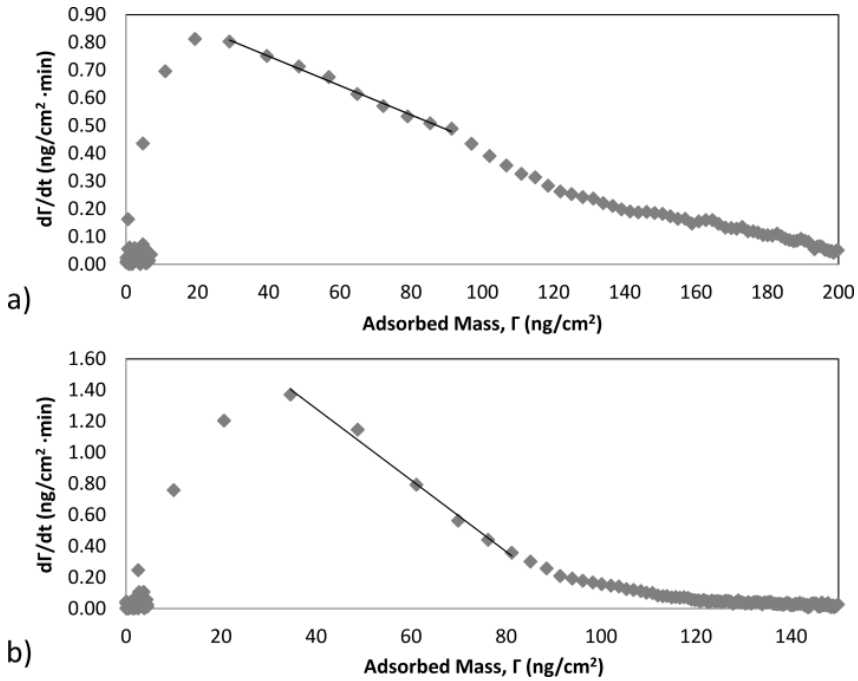

Figure D.5. The rate of adsorption versus the surface density for the first adsorption cycle of nisin at an (a) uncoated and (b) F108-coated surface. The solid line is a best fit to data in the linear, surface limited adsorption regime.

Desorption rate constants were determined in a similar fashion (Figure D.6). The two linear regions appearing in plots of adsorption rate vs. adsorbed mass indicate the presence of three adsorbed states: one that shows little resistance to elution (state 1), one with substantially greater resistance to elution (state 2), and one that is not elutable upon introduction of peptide-free buffer (state 3). During elution Eq. [2] can be written $-\frac{d\Gamma}{dt} = \left(k_{d,1}\Gamma_1 + k_{d,2}\Gamma_2\right)$, as $k_{d,3}$ =

0 initially. The slopes of the two distinct linear regions thus provide the desorption rate constants, $k_{d,1}$ and $k_{d,2}$.

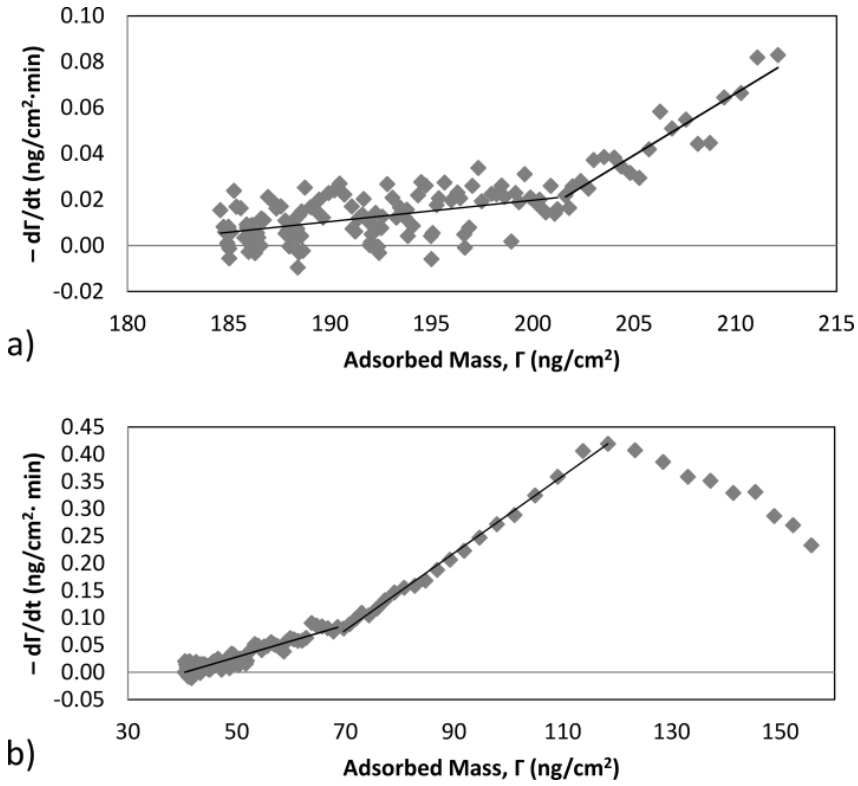

Figure D.6**.** Negative desorption rate versus surface density for the first desorption cycle of nisin at an (a) uncoated and (b) F108-coated surface. The solid lines are best fits to two linear regions, used to determine desorption rate constants as well as adsorbed states and populations.

The populations of protein in states 1-3 at the end of the first adsorption cycle can also be determined from Figure D.6, recognizing that all states are present at the onset of desorption, only states 2 and 3 are present at the intersection of the two regions, and the intersection of the low surface concentration with the *x*-intercept, i.e., where $\left.\frac{d\Gamma}{dt}\right|_{\Gamma=0}$, determines the adsorbed mass in state 3 (Figure D.7).

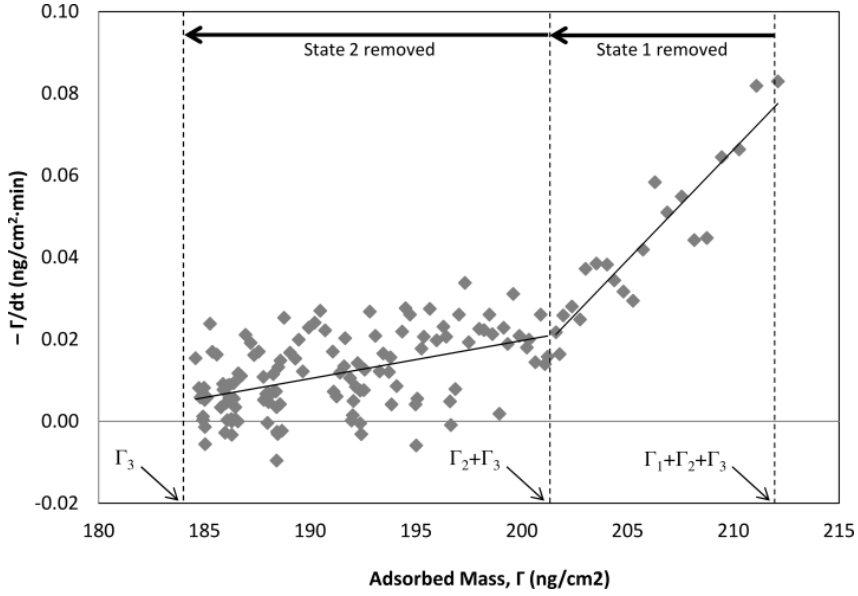

Figure D.7**.** Desorption rate versus surface density for an uncoated surface is shown as an example for desorption rate and population determination.

Once kC, and the $k_{d,i}$ and Γ_i have all been determined, Eq. [2] can be used to evaluate the modified cavity function at the onset of the second adsorption cycle for comparison to that at the same surface coverage during the first cycle, for each surface. At the onset of the second adsorption cycle, all protein is assumed to "irreversibly" adsorbed (i.e. in state 3), and Φ' can be determined at that point. Assuming that all protein is adsorbed in state 3 at the same surface coverage during the first cycle, i.e., that the first adsorbing proteins are those that are most stably adsorbed or entrapped, Φ' can be determined at this point as well.

Table D.1 lists kinetic parameters determined for the uncoated and F108-coated surfaces by the analysis summarized above. The uncoated surface showed history dependent adsorption, i.e., an increase in the modified cavity function between the first and second adsorption cycles, suggesting surface rearrangement of molecules (whether adsorbed in a primary or outer layer). The F108 surface however showed little change in the cavity function

between adsorption cycles consistent with little evidence of history dependence. Adsorption into the F108 layer was also characterized by the highest initial adsorption rate (high kC), the highest elution rate (highest $k_{d,i}\Gamma_i$) and the lowest value of Γ_3 (least amount of stably bound protein).

Table D.1. Calculated kinetic parameters for uncoated and F108-coated surfaces. Φ'_{1A} and Φ'_{2A} refer to the modified cavity function at identical surface coverages during the first and second adsorption cycle, respectively.

Parameter	Uncoated	F108-coated
kC **(ng/cm^2·min)**	0.96	2.2
$k_{d,1}$ **(min^{-1})**	0.0054	0.0071
$k_{d,2}$ **(min^{-1})**	0.001	0.003
Γ_1 **(ng/cm^2)**	10.5	85.6
Γ_2 **(ng/cm^2)**	17.4	29.3
Γ_3 **(ng/cm^2)**	184	40.4
Φ'_{1A}	0.10	0.52
Φ'_{2A}	0.27	0.59

D.4 Conclusions

Nisin adsorption to the uncoated surface showed history dependence while nisin adsorption to the F108-coated surface did not show history dependence. This was interpreted as lateral movement of peptide, whether in a primary or outer layer, resulting in cleared area for more rapid adsorption at the onset of the second cycle than recorded at the same surface coverage during the first cycle for the uncoated surface, and a lack of such rearrangement at the F108-coated surface. Nisin adsorption was not recorded at (fibrinogen-repellent) F68-coated surfaces. The lack of history dependence and high elutability characterizing nisin adsorption to the F108 layer, and the obvious lack of nisin association with the underlying surface or with the surrounding PEO chains at F68-coated surfaces, suggest nisin entrapment involves its location within the hydrophobic phase of immobilized PEO, without contacting the underlying surface. While nisin entry into the F68 brush was observed (Figure D.3), its high elutability is possibly a result of the relatively short PEO chain length afforded by immobilized F68 being insufficient to form the level of attractive associations required for entrapment.

D.5 Acknowledgments

This work was supported in part by the National Institute of Biomedical Imaging and Bioengineering (NIBIB, grant no. R01EB011567). The content is solely the responsibility of the authors and does not necessarily represent the official views of NIBIB or the National Institutes of Health.

D.7 References

[1] M. Ryder, P., K. F. Schilke, J. A. Auxier, J. McGuire, and J. A. Neff, "Nisin adsorption to polyethylene oxide layers and its resistant to elution in the presence of fibrinogen," *Journal of Colloid and Interface Science,* vol. 350, pp. 194-199, 2010.

[2] Y.-C. Tai, P. Joshi, J. McGuire, and J. A. Neff, "Nisin adsorption to hydrophobic surfaces with the PEO-PPO-PEO triblock surfactant Pluronic® F108," *Journal of Colloid and Interface Science,* vol. 322, pp. 112-118, 2008.

[3] W. T. E. Bosker, P. A. Iakovlev, W. Norde, and M. A. C. Stuart, "BSA adsorption on bimodal PEO brushes," *Journal of Colloid and Interface Science,* vol. 286, pp. 496-503, 2005.

[4] W. Norde and D. Gage, "Interaction of Bovine Serum Albumin and Human Blood Plasma with PEO-Tethered Surfaces: Influence of PEO Chain Length, Grafting Density, and Temperature," *Langmuir,* vol. 20, pp. 4162-4167, 2004.

[5] S. J. Sofia, V. Premnath, and M. E. W., "Poly(ethylene oxide) Grafted to Silicon Surfaces: Grafting Density and Protein Adsorption," *Macromolecules,* vol. 31, pp. 5059-5070, 1998.

[6] N.-P. Huang, R. Michel, J. Voros, M. Textor, R. Hofer, A. Rossi, *et al.*, "Poly(L-lysine)-g-poly(ethylene glycol) Layers on Metal Oxide Surfaces: Surface-Analytical Characterization and Resistance to Serum and Fibrinogen Adsorption," *Langmuir*, vol. 17, pp. 489-498, 2001.

[7] Y.-C. Tai, J. McGuire, and J. Neff, "Nisin antimicrobial activity and structural characteristics at hydrophobic surfaces coated wit the PEO-PPO-PEO triblock surfactant Pluronic® F108," *Journal of Colloid and Interface Science,* vol. 322, pp. 104-111, 2008.

[8] Y.-C. Tseng, T. McPherson, C. S. Yuan, and K. Park, "Grafting of ethylene glycol-butadiene block copolymers onto dimethyl-dichlorosilane-coated glass by γ-irradiation," *Biochemistry,* vol. 16, 1995.

[9] T. B. McPherson, H. S. Shim, and K. Park, "Grafting of PEO to glass, nitinol, and pyrolytic carbon surfaces by γ irradiation," *Journal of Biomedical Materials Research,* vol. 38, 1997.

[10] L. D. Unsworth, H. Sheardown, and J. L. Brash, "Protein-Resistant Poly(ethylene oxide)-Grafted surfaces: Chain Density-Dependent Multiple Mechanisms of Action," *Langmuir,* vol. 24, pp. 1924-1929, 2008.

[11] L. D. Unsworth, H. Sheardown, and J. L. Brash, "Polyethylene oxide surfaces of variable chain density by chemisorption of PEO-thiol on gold: Adsorption of proteins from plasma studied by radiolabelling and immunoblotting," *Biomaterial,* vol. 26, pp. 5927-5933, 2005.

[12] A. Higuchi, K. Sugiyama, B. O. Yoon, M. Sakurai, M. Hara, M. Sumita, *et al.*, "Serum protein adsorption and platelet adhesion on pluronic(TM)-adsorbed polysulfone membranes," *Biomaterials,* vol. 24, pp. 3235-3245, 2003.

[13] R. J. Green, M. C. Davies, C. J. Roberts, and S. J. B. Tendler, "A surface plasmon resonance study of albumin adsorption to PEO-PPO-PEO triblock copolymers," *Journal of Biomedical Material Research,* vol. 42, pp. 165-171, 1998.

[14] J. K. Dill, J. A. Auxier, K. F. Schilke, and J. McGuire, "**Quantifying nisin adsorption behavior at pendant PEO layers**," *Journal of Colloid and Interface Science,* 2013.

[15] W. Norde and C. E. Giacomelli, "BSA structural changes during homomolecular exchange between the adsorbed and the dissolved states," *Journal of Biotechnology,* vol. 79, pp. 259-268, 2000.

[16] C. F. Wertz and M. M. Santore, "Fibrinogen Adsorption on Hydrophilic and Hydrophobic Surfaces: Geometrical and Energetic Aspects of Interfacial Relaxations," *Langmuir,* vol. 18, 2002.

[17] Y. Tie, P. Ngankam, and P. R. Van Tassel, "Probing Macromolecular Adsorbed Layer Structure and History Dependence via the Interfacial Cavity Function," *Langmuir,* vol. 20, pp. 10599-10693, 2004.

[18] E. Breukink and B. de Krujiff, "Lipid II as a target for antibiotics," *Nature Reviews Drug Discovery,* vol. 5, 2004.

[19] I. Wiedemann, E. Breukink, C. van Kraaij, O. P. Kuipersi, G. Bierbaum, B. de Krujiff, *et al.*, "Specific Binding of Nisin to the Peptidoglycan Precursor Lipid II Combines Pore Formation and Inhibition of Cell Wall Biosynthesis for Potent Antimicrobial Activity," *The Journal of biological Chemistry,* vol. 276, pp. 1776-1779, 2001.

[20] A. J. M. Dreissen, H. W. van den Hooven, W. Kuiper, M. van de Kamp, H.-G. Sahl, R. N. H. Koning, *et al.*, "Mechanistic studies of lantibiotic-induced permeabilization of phospholipid vesicles," *Biochemistry,* vol. 34, pp. 1606-1614, 1995.

[21] E. Ruhr and H.-G. Sahl, "Mode of action of the peptide antibiotic nisin and influence of the membrane potential of whole cells and on cytoplasmic and artificial membrane vesicles," *Antimicrobial Agents and Chemotherapy,* vol. 27, pp. 841-845, 1985.

[22] S.-T. Hsu, E. Breukink, E. Tischenki, M. A. G. Lutters, B. de Kruijiff, R. Kaptein, *et al.*, "The nisin-lipid II complex reveals a pyrophosphate cage that provides a blueprint for novel antibiotics," *Nature Structural & Molecular Biology,* vol. 11, 2004.

[23] A. Halperin, "Polymer brushes that resist adsorption of model proteins: Design parameters," *Langmuir,* vol. 15, 1999.

[24] K. F. Schilke and J. McGuire, "Detection of nisin and fibrinogen adsorption on poly(ethylene oxide) coated polyurethane surfaces by time-of-flight secondary ion mass spectrometry (TOF-SIMS)," *Journal of colloid and Interface Science,* vol. 358, pp. 14-24, 2011.

[25] H. Salmio and D. Bruhwiler, "Distribution of amino groups on a mesoporous silica surface after submonolayer deposition of aminopropylsilanes from an anhydrous liquid phase," *Journal of Physical Chemistry,* vol. C111, 2007.

[26] A. Székács, N. Adányi, I. Székács, K. Majer-Baranyi, and I. Szendrö, "Optical waveguide light-mode spectroscopy immunosensors for environmental monitoring," *Applied Optics,* vol. 48, 2009.

[27] J. Cleveland, T. J. Monteville, I. F. Nes, and M. L. Chikindas, "Bacteriocins: safe, natural antimicrobials for food preservation," *International Journal of Food Microbiology,* vol. 71, pp. 1-20, 2001.

[28] P. Appenini and J. H. Hotchkiss, "Review of antimicrobial food packaging," *Innovative Food Science & Emerging Technologies,* vol. 3, pp. 113-126, 2002.

[29] I. Wiedemann, E. Breukink, C. van Kraaij, O. P. Kuipers, G. Bierbaum, B. de Kruijff, *et al.*, "Specific binding of nisin to the peptidoglycan precursor lipid II combines pore formation and inhibition of cell wall biosynthesis for potent antibiotic activity," *Journal of Biological Chemistry,* vol. 276, pp. 1772-1779, January 19, 2001 2001.

[30] Y.-C. Tai, P. Joshi, J. McGuire, and J. A. Neff, "Nisin adsorption to hydrophobic surfaces coated with the PEO–PPO–PEO triblock surfactant Pluronic® F108," *Journal of Colloid and Interface Science,* vol. 322, pp. 112-118, 2008.

[31] Y.-C. Tai, J. McGuire, and J. A. Neff, "Nisin antimicrobial activity and structural characteristics at hydrophobic surfaces coated with the PEO–PPO–PEO triblock surfactant Pluronic® F108," *Journal of Colloid and Interface Science,* vol. 322, pp. 104-111, 2008.

[32] M. P. Ryder, K. F. Schilke, J. A. Auxier, J. McGuire, and J. A. Neff, "Nisin adsorption to polyethylene oxide layers and its resistance to elution in the presence of fibrinogen," *Journal of Colloid and Interface Science,* vol. 350, pp. 194-199, 2010.

[33] Y. Tie, C. Calonder, and P. R. Van Tassel, "Protein adsorption: Kinetics and history dependence," *Journal of Colloid and Interface Science,* vol. 268, pp. 1-11, 2003.

[34] K. C. Popat, R. W. Johnson, and T. A. Desai, "Characterization of vapor deposited thin silane films on silicon substrates for biomedical microdevices," *Surface and Coatings Technology,* vol. 154, pp. 253-261, 2002.

[35] T. McPherson, A. Kidane, I. Szleifer, and K. Park, "Prevention of protein adsorption by tethered poly(ethylene oxide) layers: Experiments and single-chain mean-field analysis," *Langmuir,* vol. 14, pp. 176-186, Jan 1998.

[36] J. J. Ramsden, "Porosity of pyrolysed sol-gel waveguides," *Journal of Materials Chemistry,* vol. 4, pp. 1263-1265, 1994.

[37] J. A. De Feijter, J. Benjamins, and F. A. Veer, "Ellipsometry as a tool to study the adsorption behavior of synthetic and biopolymers at the air–water interface," *Biopolymers,* vol. 17, pp. 1759-1772, 1978.

[38] L. D. Unsworth, H. Sheardown, and J. L. Brash, "Protein-resistant poly(ethylene oxide)-grafted surfaces: Chain density-dependent multiple mechanisms of action," *Langmuir,* vol. 24, pp. 1924-1929, 2008/03/01 2008.

[39] C. Calonder, Y. Tie, and P. R. Van Tassel, "History dependence of protein adsorption kinetics," *Proceedings of the National Academy of Sciences of the United States of America,* vol. 98, pp. 10664-10669, September 11, 2001 2001.

[40] C. Calonder and P. R. Van Tassel, "Kinetic Regimes of Protein Adsorption," *Langmuir,* vol. 17, pp. 4392-4395, 2001/07/01 2001.

[41] O. Joshi, H. J. Lee, J. McGuire, P. Finneran, and K. E. Bird, "Protein concentration and adsorption time effects on fibrinogen adsorption at heparinized silica interfaces," *Colloids and Surfaces B: Biointerfaces,* vol. 50, pp. 26-35, 2006.

[42] M. Lakamraju, J. McGuire, and M. Daeschel, "Nisin Adsorption and Exchange with Selected Milk Proteins at Silanized Silica Surfaces," *Journal of Colloid and Interface Science,* vol. 178, pp. 495-504, 1996.

[43] A. Halperin, "Polymer brushes that resist adsorption of model proteins: Design parameters," *Langmuir,* vol. 15, pp. 2525-2533, 1999/03/01 1999.

[44] S. R. Sheth and D. Leckband, "Measurements of attractive forces between proteins and end-grafted poly(ethylene glycol) chains," *Proceedings of the National Academy of Sciences of the United States of America,* vol. 94, pp. 8399-8404, August 5, 1997 1997.

[45] A. Halperin, "Compression induced phase transitions in PEO brushes: the *n*-cluster model," *European Physical Journal B: Condensed Matter and Complex Systems,* vol. 3, pp. 359-364, 1998.

[46] T. Hu and C. Wu, "Clustering induced collapse of a polymer brush," *Physical Review Letters,* vol. 83, pp. 4105-4107, 1999.

[47] M. Wagner, F. Brochard-Wyart, H. Hervet, and P. Gennes, "Collapse of polymer brushes induced by n-clusters," *Colloid and Polymer Science,* vol. 271, pp. 621-628, 1993.

[48] H. Lee, D. H. Kim, K. N. Witte, K. Ohn, J. Choi, B. Akgun, *et al.,* "Water Is a Poor Solvent for Densely Grafted Poly(ethylene oxide) Chains: A Conclusion Drawn from a Self-Consistent Field Theory-Based Analysis of Neutron Reflectivity and Surface Pressure–Area Isotherm Data," *Journal of Physical Chemistry B,* vol. 116, pp. 7367-7378, 2012.